Exploring Chiral Symmetry Breaking and Chiral Amplification in Conglomerate Crystals

Ziqiao Zhong

A Thesis
in
The Department
of
Chemistry and Biochemistry

Presented in Partial Fulfillment of the Requirements
For the Degree of Master of Science (Chemistry) at

Concordia University
Montreal, Quebec, Canada

Fall, 2023

CONCORDIA UNIVERSITY

School of Graduate Studies

This is to certify that the thesis prepared

By: Ziqiao Zhong

Entitled: Exploring Symmetry Breaking and Chiral Amplification in Conglomerate Crystals

and submitted in partial fulfillment of the requirements for the degree of

Master of Science (Chemsitry)

complies with the regulations of the University and meets the accepted standards with respect to originality and quality.

Signed by the final Examining Committee:

_____ Chair

Prof. Ingo Salzmann

_____ Examiner

Prof. Yves Gélinas

_____ Examiner

Prof. Ashlee Howarth

_____ Supervisor

Prof. Louis Cuccia

Approved by _____

Chair of Department or Graduate Program Director

_____ 2023 _____

Dean of Faculty

ABSTRACT

Exploring Symmetry Breaking and Chiral Amplification in Conglomerate Crystals

Ziqiao Zhong

Conglomerate crystallization, also known as spontaneous resolution, occurs when molecules crystallize in a non-centrosymmetric space group.[1] Both racemic and achiral building blocks can crystalize as conglomerates to form chiral crystals. The chiral outcome (*i.e.* the distribution of left- versus right-handed crystals) can be stochastic or non-stochastic depending on the environment and crystallization conditions.[2, 3] Herein the influence of primary and secondary nucleation in the conglomerate crystallization of benzil was explored. The results indicate that chiral amplification is favored under conditions that promote secondary nucleation. The complete and controlled chiral amplification of benzil was confirmed *via* attrition-enhanced deracemization (*i.e.* Viedma ripening) in under 2 hours, while the Viedma ripening of decacyclene was also demonstrated over a period of *ca*. 15 days. Viedma ripening provides non-equilibrium conditions that promote secondary nucleation through enantiomer-specific oriented attachment non-classical crystal growth.

Non-stochastic conglomerate crystallization from achiral building blocks is surprisingly common and not well understood. Herein, one of the earliest examples was investigated, where an overwhelming imbalance (134 right-handed crystals, 5 left-handed crystal) was confirmed in the conglomerate crystallization of magnesium sulfate heptahydrate ($MgSO_4 \cdot 7H_2O$), epsomite.[4] In such cases, it is believed that hidden chiral (cryptochiral) environments that influence the primary crystal nucleation are to blame. As such, chiral additives (L- and D-asparagine) were used to influence the mirror symmetry breaking in epsomite crystallization. The chiral distribution resulting from the conglomerate crystallization of achiral molecules is fascinating since it may provide insight regarding polymorphism and the outstanding question of the origin of biological homochirality.

DEDICATION

I would like to especially show my gratefulness to my supervisor, Dr. Louis A. Cuccia, who has provided advice, suggestions, and resources for me in my studies. It is my great honor to join this lab and meet with so many wonderful people who supported me and guided me not just in science but in my life. You are a good supervisor.

I am happy to learn from Dr. Jeanne Paquette, Dr. D. Scott Bohle and Dr. Robert A Pascal, Jr., who provided me with help in my project and studies. I want to thank Reajean Sivakumar, Munendra Yadav, Cameron Lennox, Thi Phuong Thao Nguyen and Evelyn Human for cooperating in my studies. I also thank my committee members, Dr. Ashlee Howarth and Dr. Yves Gélinas for the guidance and support.

I would like to thank you Kwan Ming Tam, who encouraged me to apply for graduate studies. You are a great but humble person, hardworking and intelligent. You are such a great person for me as a role model and a friend. Thank you for providing me with help when I was frustrated.

Aida, my best friend in my life, thank you for being an angel to me. You are brave, kind, and sweet. I enjoy every moment I spent with you. I am grateful to have you study with me during my whole undergraduate period. I learnt how to be a better person from your positive attitude towards life. You are thoughtful and decisive in your actions. I enjoy hearing about your new projects, your dreams, your life. I can always get some inspiration from you.

I would like to thank everyone I met in the lab. Louis, you are harsh and smart, but you always say things with good intentions. I understand I can improve and thank you for guiding me in this direction. Thank you, Shirley, for being kind and tolerating my faults. Thank you, Greg, you are the best colleague I have ever worked with, helpful, considerate, and responsible. Thank you, Serhish, your presentations are so wonderful, and I am so glad to learn from you. Thank you, Karim, you are helping so much in the benzil study. It is not easy to work and study at the same time, I learn a lot from interacting with you as well. Thank you, Renata, the favorite of everybody. Thank you, Tsion, you have a tiny body, but you have a great heart. Thank you for helping me with my project even during the weekends, and taking care of experiments when I was absent. Thank you, Natalia, even if you are always in the other room, I am so happy to have your companionship.

I need to thank you, Thomas. You take care of me, and give me help on my plotting, help me fix the cross reference. Thank you for going through this with me. I am grateful to have you in my life.

Table of Contents

List of Figures

List of Tables

1 Introduction

1.1 Research Overview

Homochirality is a crucial property found in the fundamental building blocks of chemistry and biochemistry molecules.[5] The significance of studying chiral materials in a homochiral form has become even more important following the tragic incidents involving thalidomide, where birth defects were caused by one specific enantiomer of this drug.[6, 7] Despite its importance, the obtaining of homochiral materials from racemic mixtures continues to present significant challenges, since both enantiomers have the same melting points, densities, and solubilities.[8]

The study of the chiral distribution of conglomerate crystals has constantly developed along with the understanding of chirality itself beginning in the 19 century.[9] Conglomerate crystallization of racemic mixtures yields equal amounts of each enantiomer, as Pasteur observed with sodium ammonium tartrate monohydrate in 1848.[10] It is intuitive that a 50:50 chiral distribution of a racemic mixture is retained upon crystallization to the solid state. However, it is not necessarily true in the conglomerate crystallization of achiral building blocks. During crystallization, the degree of primary and secondary nucleation can influence the emerging solid state chirality *via* classical and/or non-classical crystal growth.[11, 12] The chirality of conglomerate crystals from achiral molecules originate from either a locked chiral conformation in the solid state (**Section 1.2**) or from chiral packing in non-centrosymmetric Sohncke space groups (**Section 1.3**).[8, 13, 14] The resulting chiral distribution in the conglomerate crystallization of achiral molecules is fascinating, since it may provide insight into the outstanding question of the origin of biological homochirality.[5]

There are some common terms used throughout this thesis for describing the chiral distribution of chiral materials. Crystals or molecules sharing the same chirality are homochiral. If there is an equal population of chiral molecules or crystals, this is known as a racemic mixture. Two opposite homochiral materials mixed in any ratio not equal to 1:1 is known as a scalemic mixture. The ratio of a chiral mixture can be quantified by the concept of enantiomeric excess, which describes the mole or weight fraction (where F(+) + F (-) = 100%) of one chiral species.[15] Enantiomer excess can be calculated according to **Equation 1** as shown below:

Equation 1. The equation for calculating enantiomeric excess.[15]

$$\text{ee}\% = \frac{|\text{F}(+) - \text{F}(-)|}{|\text{F}(+) + \text{F}(-)|} \times 100\%$$

This thesis explores both the symmetry breaking and chiral amplification of conglomerate crystals originating from achiral building blocks. Specifically, the historic symmetry breaking of epsomite was explored in the absence and presence of chiral additives. The chirality of benzil and decacyclene crystal suspensions were explored under various conditions, specifically applying attrition and temperature control. More information about those materials and their solid-state chirality is provided in **Chapter 2** and **3**. **Chapter 4** investigates the non-stochastic crystallization of epsomite and the use of chiral additives as a tool to direct mirror symmetry breaking. Ultimately, the research described in this thesis focuses on the fundamental understanding of conglomerate crystallization which is beneficial to future developments in chiral studies.

1.2 The chirality of molecules

According to IUPAC, chirality is "the geometric property of a rigid object (or spatial arrangement of points or atoms) of being non-superimposable on its mirror image. If the object is superposable on its mirror image the object is described as being achiral."[15] It is an important feature particularly in the fields of chemistry and biochemistry. Chirality is ubiquitous in the fundamental building blocks of life, like sugars, amino acids, and lipids.[16] A molecule is achiral if it lacks an improper axis (S_n) which is a combination of rotation and reflection.[15, 17] More simply, a molecule is chiral if it is non-superimposable with its mirror image.

Many systems of nomenclature have been developed for differentiating different stereoisomers. The Cahn Ingold Prelog Priority Rules (CIP rules) are used in labeling isomer with a stereogenic center.[15] Taking asparagine as an example, there is only one carbon with 4 different substituents. The substituents are ranked by conventional rules based on atomic number and connectivity. When the lowest priority group ④ is pointing back, the compound has the R configuration when substituents ① to ③ move in a clockwise direction, and it has the S configuration when substituents ① to ③ move in a counterclockwise direction (**Figure 1**).[15]

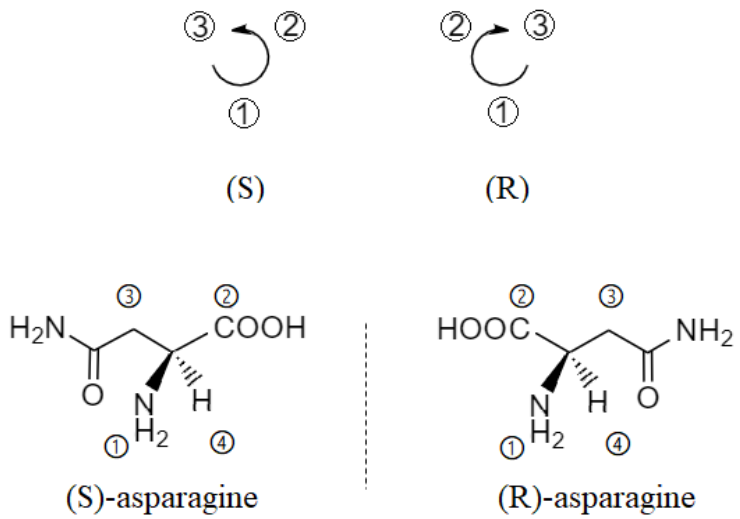

Figure 1. An example of the Cahn Ingold Prelog priority rules and Fischer nomenclature.

S-asparagine and R-asparagine are more commonly referred to in the Fischer nomenclature as L-asparagine and D-asparagine, respectively. Here, the vertical lines project inwards and the horizontal lines project outwards and the most oxidized carbon is at the top position in the Fischer projection with the longest carbon chain vertical. [17, 18] The L-designator is assigned when the -H group is to the right and the D-designator is assigned when the -H is to the left at the highest numbered stereogenic center (*i.e.* lowest chiral carbon of the chain, **Figure 2**).[19]

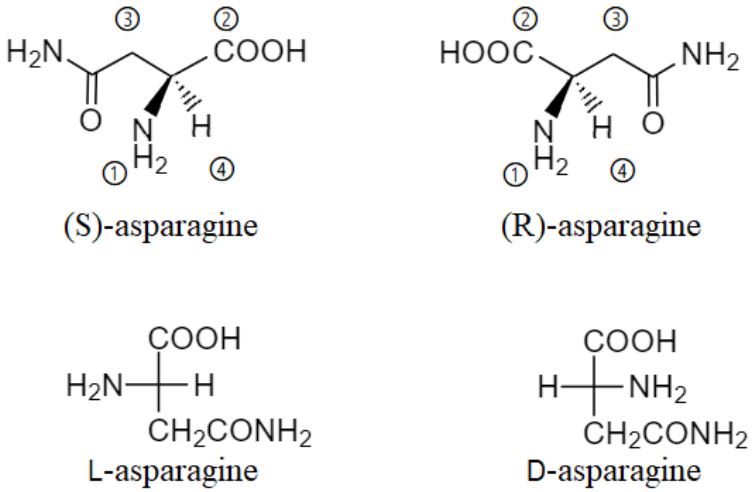

Figure 2. The enantiomeric pair of asparagine labeled with both CIP and Fischer nomenclature.

Tartaric acid is an important molecule in the early development of chiral studies.[20] The enantiomeric pair of tartaric acid molecules are non-superimposable mirror images to each other, and both have 2 stereogenic centers with the same configuration (**Figure 3**).

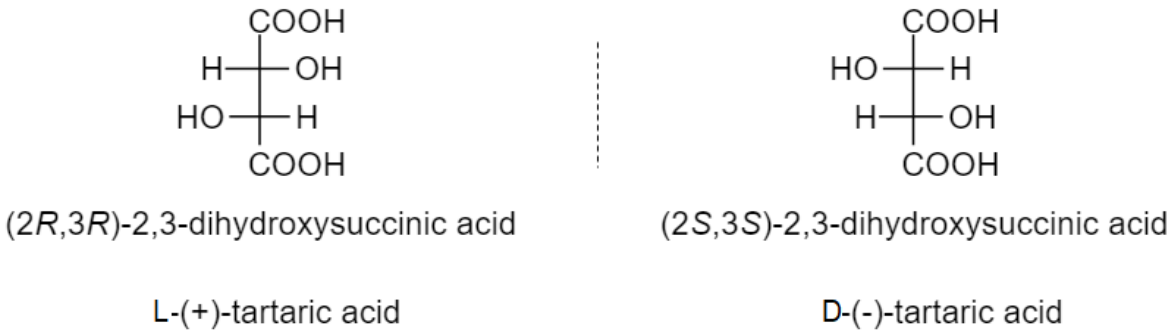

Figure 3. The enantiomeric pair of tartaric acid labeled with CIP and Fischer nomenclature.

The form of tartaric acid with an internal plane of symmetry is achiral and is designated as a meso-compound (**Figure 4)**.[15] The absolute configuration assigned in Fischer nomenclature (D/L) is frequently mixed up with the shortened form of dextrorotatory (*d*) or levorotatory (*l*). The latter refers to the sign of rotation of plane-polarized light as being positive (+) or negative (-), respectively.[15]

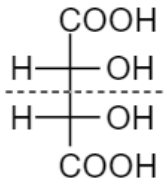

(2*R*,3*S*)-2,3-dihydroxysuccinic acid

DL-tartaric acid

Figure 4. This meso-isomer of tartaric acid has an internal plane of symmetry and is achiral.

Another type of chirality that some molecules can have is helical chirality. Helicity can describe the chirality of a helical, propeller, or screw-shaped molecule.[15] Intramolecular interactions and hinderance between atoms can drive certain compounds to adopt non-planar helical conformations. A molecule with a right-handed arrangement of atoms moving from front to back is designated as a P helix (plus) and a molecule with a left-handed arrangement of atoms moving from front to back is designated as an M helix (minus) (**Figure 5)**.[15]

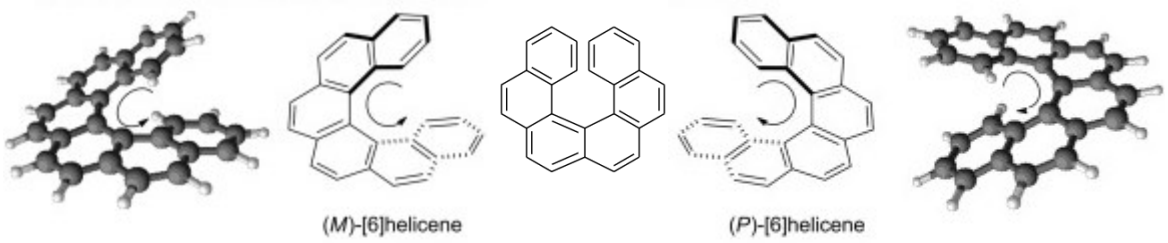

Figure 5. The enantiomeric pair of [6]-helicene with corresponding stereodescriptors.[8]

Achiral molecules can also adopt chiral conformations (**Figure 6**). [8, 21] For example, benzil can be represented in a flat achiral conformation, but through rotation about the central single bond can adopt chiral conformations. If the barrier for rotation in solution is low, as is the case for benzil, the average of all conformations in solution will be achiral. Benzil crystallizes in the chiral space groups $P3_121$ or $P3_231$ thus forming conglomerate crystals.[22] Benzil adopts a locked chiral conformation in the solid state forming homochiral (+)-crystals with benzil in the P-conformation (space group $P3_121$), and homochiral (-)-crystals with benzil in the M-conformation (space group: $P3_221$) (**Figure 6**).[22, 23]

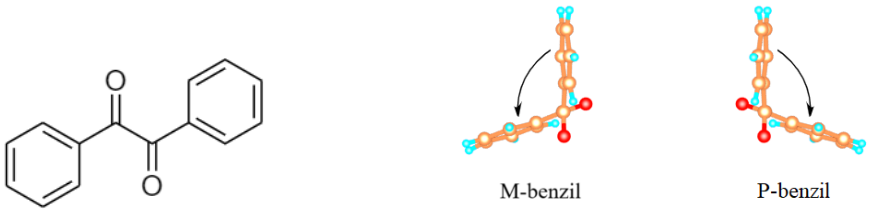

Lewis structure Chiral conformations of benzil

Figure 6. Benzil is an achiral molecule fixed at a non-centrosymmetric conformation in the solid state (space group $P3_121$ and $P3_221$).[23]

There are also examples of molecules having bonds with restricted rotation, where separation of enantiomeric conformations in solution is possible. This class of stereoisomers are known as atropisomers, where the half-life of racemization depends on the energy barrier of the bond rotation which restricts the conformational conversion from one enantiomer to the other.[15] For example, tri-*o*-thymotide (host) can form inclusion clathrate crystals with solvent molecules (guest) to form chiral atropisomeric clathrates.[24] The chiral tri-*o*-thymotide-benzene clathrate requires 16 kCal/mol to racemize in chloroform and the racemization half-life is 2.4 minutes.[24]

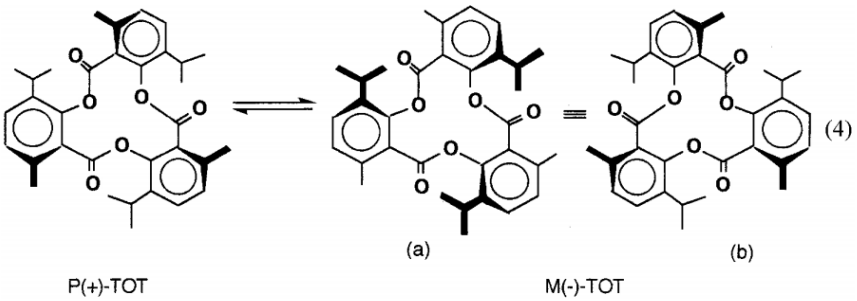

Figure 7. P- and M- coformations of tri-*o*-thymotide (T*o*T) in the T*o*T-benzene clathrate. The racemization half-life of the T*o*T-benzene clatherate is *ca.* 2.4 minutes in chloroform.[24]

1.3 The chirality in crystals

Space groups define the symmetrical relationship between atoms and molecules within crystals.[8] There are 230 space groups in total, which can be divided into 3 classes according to the type of symmetry operations they have. Most of the space groups, 165 out of 230 space groups, are Class I having an improper axis, which makes the crystals in these space groups achiral.[1] There are 11 pairs of space groups that have an asymmetric structure, which are the 22 chiral space groups in the Class II.[1] The remaining 43 space groups in the Class III are also achiral and have only proper rotations and 2-fold screw rotation.[1] The space groups in the latter two classes are non-centrosymmetric since those space groups do not have an inversion center between atoms.[1, 8] In **Figure 8**, all 65 space groups (Sohncke space group) that belong to the last two classes are listed on the left side, and the chiral space groups are listed on the right side. Any crystal crystallization in one of these Sohncke space groups is chiral, regardless of whether the building blocks are chiral or achiral.[1, 25]

P 1
P 121, *P* 12_11, *C* 121
P 222, *P* 222_1, *P* 2_12_12, *P* $2_12_12_1$,
C 222_1, *C* 222, *F* 222, *I* 222, *I* $2_12_12_1$
P 4, *P* 4_1, *P* 4_2, *P* 4_3, *I* 4, *I* 4_1
P 422, *P* 42_12, *P* 4_122, *P* 4_12_12, *P* 4_222, *P* 4_22_12,
P 4_322, *P* 4_32_12, *I* 422, *I* 4_122
P 3, *P* 3_1, *P* 3_2, *R* 3
P 312, *P* 321, *P* 3_112, *P* 3_121, *P* 3_212, *P* 3_221, *R* 32
P 6, *P* 6_1, *P* 6_5, *P* 6_2, *P* 6_4, *P* 6_3
P 622, *P* 6_122, *P* 6_522, *P* 6_222, *P* 6_422, *P* 6_322
P 23, *F* 23, *I* 23, *P* 2_13, *I* 2_13
P 4_32, *P* 4_232, *F* 432, *F* 4_132, *I* 432,
P 4_332, *P* 4_132, *I* 4_132

P 4_1, *P* 4_3
P 4_122, *P* 4_322
P 4_12_12, *P* 4_32_12
P 3_1, *P* 3_2
P 3_112, *P* 3_212
P 3_121, *P* 3_221
P 6_1, *P* 6_5
P 6_2, *P* 6_4
P 6_122, *P* 6_522
P 6_222, *P* 6_422
P 4_332, *P* 4_132

Figure 8. 65 non-centrosymmetric Sohncke space groups. The 11 pair of chiral space groups are on the right.[1]

1.4 Conglomerate crystallization

Obtaining homochiral material is an ongoing challenge. Even though conglomerate crystals can spontaneously resolve, it is still difficult to separate the two enantiomorphic populations of crystals. There are three main strategies to achieve enantioenrichment or homochirality that involve conglomerate crystallization in either chiral or achiral systems.[26] The most traditional yet challenging method is manually resolving conglomerate crystals as Louis Pasteur carried out in the resolution of sodium ammonium tartrate monohydrate (**Section 1.4.2**).[27] A more common means to obtain enantioenrichment in conglomerate crystals is by introducing seed crystals of the desired chirality in the mother liquor.[28] In other words, the seeds of the desired chiral species introduced into a saturated racemic solution promotes crystal growth with the same chirality while the solution becomes enriched in the opposite chirality. By repeating this process, it is possible to obtain enantioenriched or homochiral material. When starting from a racemic mixture of chiral molecules, the maximum theoretical yield of each enantiomer is 50% (**Section 1.4.3**). However, in the case of conglomerate crystallization from achiral building blocks, it becomes possible to obtain 100% yield of homochiral crystals (**Section 1.4.3** and **Section 1.4.4**).[29] A third method is the non-equilibrium deracemization of conglomerate crystals known as Viedma ripening.[30] This chiral amplification process is a relatively new solid-state process that takes advantage of solution state racemization (or the loss of chirality in solution) combined with non-classical crystal growth under attrition, temperature cycling, or solvent cycling conditions to obtain a homochiral population of crystals (**Section 1.4.5)**.[30-32]

1.4.1 Conglomerate crystals

Conglomerate crystallization is a process of forming homochiral crystals spontaneously from racemic mixtures or, in some cases, from achiral molecules. Conglomerate crystallization is often referred to as spontaneous resolution which can facilitate enantioenrichment as exemplified by the first example of separating homochiral molecules from racemic mixture in history: the manual resolution of sodium ammonium tartrate monohydrate by Louis Pasteur in 1848.[27, 33] More recently, conglomerate crystals have been used to obtain enantioenriched products in certain asymmetric autocatalytic reactions and Diels-Alder reactions.[34-37]

The great potential of conglomerate crystals in chiral studies has often been overlooked. Many chemists did not remark that newly reported crystal structures were conglomerate crystals.[38] The 1981 book '*Enantiomers, Racemates, and Resolutions*' identified 1300 conglomerate structures and indicated that both racemic molecules and achiral molecules should have a similar possibility of 5-10% to crystallized as conglomerate crystals.[39] The percentage of forming conglomerate crystals with achiral molecules can further increase by pairing with another

component to form two-component crystals, for examples the cocrystals of benzophone derivatives or 2,4,6-triisopropylbenzophenone derivatives have 24% and 33% probability of conglomerate formation, respectively.[40, 41]

In 2005, a Cambridge Structural Database (CSD) (1988 edition) survey by Matsuura et *al*., of 190,000 organic and organometallic compounds estimated the percentage of chiral crystals from achiral molecules to be 8%.[41] More investigations into the building blocks of conglomerate crystals continue as the database is growing. The Inorganic Crystal Structure Database (ICSD from FIZ Karlsruhe-2020) is composed of over 200,000 inorganic crystal structures and the Cambridge Crystal Structure Database (CCSD) contains more than 1.1 million structures (CSD version 3.41, November 2019). Both databases show that many inorganic salts crystallize as conglomerate crystals.[26, 42]

This estimate for conglomerate crystallization rose from 8% to 9.5% in the survey of Rekis et *al*., published in 2020.[38] Rekis searched 82,965 chiral structures and 95,959 achiral structures from the CSD (Feb 2019) and expected that there should be 4281 conglomerates from chiral molecule. The conglomerates from chiral molecules should have a similar 9.5% ratio as the conglomerates from achiral molecules (9128 out of 95,959), which suggests that there are 38% of chiral organic conglomerate crystals hidden in the CSD.[26, 38] This encouraged Walsh *et al.* to expand the search for chiral conglomerates in the database. By 2023, they identified 343 chiral conglomerate crystals and 898 achiral conglomerate crystals from 108,000 new crystal entries between 2020 and 2021.[26, 43]

The space groups that are preferentially populated with conglomerate crystals is also another important topic. The ICSD from FIZ Karlsruhe-2020 reported $P6_3$, $P2_12_12_1$, $P2_13$, $P3_121$, and P1 are the most common space groups among conglomerate crystals in decreasing order.[44] A report of the CSD (November 2021, version 5.43) listed the trend of popular space groups in decreasing order from chiral conglomerate crystals as: $P2_12_12_1$, $P2_1$, C2, P1, $P2_12_12$, $P4_12_12_1$/$P2_32_12_1$, $P3_1$/ $P3_2$, and $P4_1$/ $P4_3$. [26, 43] The most popular space groups among chiral conglomerates are the $P2_12_12_1$ and $P2_1$ space groups, which account for about 52% and 34% of conglomerate crystals, respectively.[43]

1.4.2 Triage

The asymmetric appearance of mirror image conglomerate crystals allows for the possibility of visual separation of enantiomorphic crystals (*i.e.* resolution by triage or Pasteurian resolution) to be possible.[45] The manually resolution of conglomerate crystals depends on the presence of hemihedral faces, the crystal faces that do not have a corresponding parallel face on the opposite side of crystal.[46] Some conglomerate crystals can be

resolved by the presence of hemihedral faces but it is challenging.[20] However, crystal morphology is not only govern by the lattice geometry, but also by the speed of face growth related to other environmental factors during the crystallization.[47] Crystal habit and morphology can vary due to crystallization temperature, solvent, mixing, supersaturation and impurities.[48] It should be noted that resolution by triage is quite rare because of the painstaking process of manual sorting individual crystals. As a result, there are only a few examples of resolution by triage reported in the literature (examples listed in **Table 1**). [45, 47]

Table 1. Examples of crystals displaying hemihedrism.

Building blocks	Name	Space Group	Crystallization Type	Reference
Achiral	Magnesium sulfate heptahydrate	$P2_12_12_1$	Non-stochastic	[49]
Achiral	Sodium dihydrogen phosphate	$P\ 2_1/c$	Stochastic	[50, 51]
Achiral	Quartz	$P3_121$, $P3_221$	Stochastic	[52, 53]
Achiral	Sodium chlorate	$P2_13$	Stochastic	[54, 55]
Achiral	Sodium bromate	$P2_13$	Stochastic	[54, 55]
Achiral	Coordination Framework Augsburg-1 (CFA-1)	P321	Stochastic	[56]
Achiral	$[M(H_3L)](NO_3)_2$•MeOH M=Mn, Fe, Co, Ni, Zn	$P2_12_12_1$	Stochastic	[57]
Achiral	Wedekind–Fock–Havinga salt $(Me(Et)N^+(All)PhI^-$ •$CHCl_3)$	$P2_12_12_1$	Stochastic	[58]
Achiral	Potassium bichromate	P1	Dominant with right-handed crystal	[59]
Achiral	Lithium sulphate monohydrate	$P2_1$	Not reported	[60, 61]
Achiral	Cinnabar	$P3_121$, $P3_221$	Not reported	[54]
Achiral	1,2-Bis(N-benzoyl-N-methylamino)benzene	$P2_12_12_1$	Stochastic	[62, 63]
Racemic	Sodium ammonium tartrate monohydrate	$P2_12_12_1$	Stochastic	[33]
Racemic	*p*-toyl imide and *n*-tosylimides derivatives	$P2_12_12_1$	Not reported	[64]
Racemic	Sucrose (Cane sugar)	P2	Not reported	[65]
Racemic	Camphoric acid	$P2_1$	Not reported	[54]
Racemic	Camphomethylic acid	$P2_1$	Not reported	[54]
Racemic	Camphoethylic acid (camphor)	$P2_12_12_1$	Not reported	[54]

Building blocks	Name	Space Group	Crystallization Type	Reference
Racemic	Ammonium salt methyl ethyl allyl anilinium iodide	$P2_12_12_1$	Stochastic	[54, 66]
Racemic	Lactose	$P2_1$	Not reported	[67, 68]
Racemic	Malic acid monohydrate	$P2_12_12_1$	Not reported	[54]
Racemic	Asparagine	$P2_12_12_1$	Not reported	[54]
Racemic	Quinic acid	$P2_1$	Not reported	[54]
Racemic	Morphine monohydrate	$P2_12_12_1$	Not reported	[54]
Racemic	Hydroveratroin	$P6_2$	Stochastic	[69]
Racemic	Formyl-*dl*-neomenthylamine	N/A	Stochastic	[70]
Racemic	Inclusion compound of β-lactam and 4-Oxoazetidine-2-yl benzoate	$P2_12_12_1$	Varied from 98% ee to 8% ee, depending on the host-guest ratio	[71]
Racemic	$[(CH_3)_2NH_2]_{10}[Hf(PW_{11}O_{39})_2]\bullet 10H_2O$	$P2_1$	Stochastic	[72]
Racemic	Complex of 1,1'-binaphthyl-2,2'-dicarboxylic acid and pyrazoles	$P2_1$	Stochastic	[73]

As far back as 1795, Adrien-Marie Legendre related 'symmetry' in the crystallography domain. In 1815 the French crystallographer, René-Just Haüy noticed the asymmetry of quartz crystals and speculated that the external asymmetric appearance of the crystal is related to the internal molecular structure (**Figure 9**).[74, 75] For this reason, new terminology for describing the symmetry of crystals emerged. For example, hemihedral (hemihedry), tritohedral (tritohedry), and tetartohedral (tetartohedry) refer to crystals where only half, one-third, or one-quarter of particular faces are present, respectively.[74, 75] In 1848, Louis Pasteur used hemihedral faces in the study of sodium ammonium paratartrate and related it to isomerism. He showed that optically inactive sodium ammonium paratartrate is a mixture of two optically active molecules.[33, 74] He deduced that the constituent molecules in sodium ammonium paratartrate had the same chemical composition but their chemical structures were mirror images of each other.[33, 76] When sodium ammonium paratartrate crystallizes as a conglomerate, an equal population of left-handed and right-handed crystals were obtained. Pasteur manually separated the crystals based on the hemihedral faces and isolated the (-)-tartaric acid and (+)-tartaric acid and measured their equal but opposite optical rotation.[77] Pasteur reasoned that the opposite rotation of the two solutions indicated that the molecules were not identical but were mirror images of each other and he called this 'molecular dissymmetry'.[77]

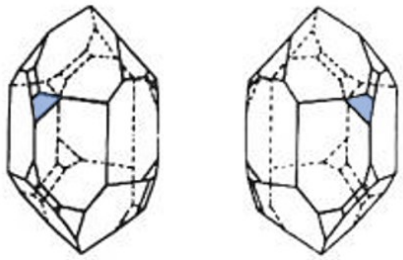

Figure 9. Mirror image quartz crystals with hemihedral faces highlighted. [53, 78]

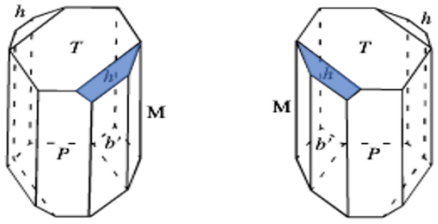

Figure 10. The non-symmetric morphology of sodium ammonium tartrate monohydrate crystals with hemihedral faces highlighted.[76]

On the other hand, an equal mixture of both crystals gave an optically inactive solution successfully proving his hypothesis that the "two species of crystals represent two distinct salts from which two different acids can be extracted".[77] With more examples of chiral crystals with asymmetric appearance recorded, Pasteur recognized that an asymmetric pair of crystals do not necessarily originate from an asymmetric pair of molecules.[79] He noted that *the asymmetry in the crystal can also come from the structure of the crystal, but not necessarily the molecule itself*.[79]

There are many methods that can distinguish crystal chirality based on different characteristics, such as, crystal morphology, crystal structure, or optical activity.[80] During the 19 century, resolution of chiral crystals relied mainly on optical activity and/or hemihedrism (*i.e.* identifying non-symmetrical faces in crystal morphology).[27, 81] X-ray crystallography, polarized light microscopy, and circular dichroism (CD) are effective modern methods for differentiating crystal chirality.[8]

One of the key optical properties allowing for the investigation of crystal chirality is birefringence. When light encounters an optically active crystal, the incident light ray is split into two rays: left-handed circularly polarized light (LCP) and right-handed circularly polarized light (RCP).[82] Each of these circularly polarized light rays has different velocities and directions.[82, 83] With the help of a polarized filter, the rotation of plane-polarized light causes a corresponding color change due to the optical activity of the crystal.[82] However, polarized filters work better with uniaxial crystals, where there is only one optic axis and a single polarization direction.[82, 84] For

crystals with more than one optic axis, the orientation of the optic axes is not fixed and may not align with the fixed polarization direction of the filter.[8, 83] As a result, the light would have more complex behavior within these types of crystal.[8] Similar problems occur in polarimetry methods, which rely on the same theory for optical activity measurements.[8, 85]

Circular dichroism spectroscopy relies on differential absorption of LCP and RCP light.[8, 85] This method is more sensitive and quantitative compared to observing chiral crystals using a polarized filter.[8] However, CD spectroscopy depends on the presence of a chromophore.[86]

X-ray diffraction (XRD) is a direct method for obtaining asymmetric information of chiral crystals.[8, 85] This method can obtain the absolute configuration of chiral crystals. The Bragg diffraction of a left-handed and right-handed crystal is identical.[87] However, when diffraction occurs near the absorption edge of a heavy atom, the difference between diffracted waves can lead to a change of intensity depending on the chirality of the structure, X or $\overline{X}$ (**Equation 2**).[8, 64] Heavier atoms are required in the structure in order to be able to determine absolute configuration.

Crystals with non-centrosymmetric structures that grow together having a mirror image of the atomic arrangement are known as inversion twins.[8] The Flack parameter (x) is an efficient method of defining the absolute configuration of a crystal (or the degree of twinning) (**Equation 2**). In other words, it determines the proportion of an oriented crystal structure X and its inverted structure $\overline{X}$ (x = 0 or 1) or both structures C in a mixed crystal ($0 < x < 1$); **Equation 2**.[8, 88] Assuming the structure C is composed of only structure X or the inverted structure $\overline{X}$, the Flack parameter (x) is 0 or 1, respectively. [89] If the crystal has a perfect inversion twin structure (*i.e.* the structure is equally populated with both structure X and structure $\overline{X}$ in a crystal, the flack parameter, x, would be 0.5.[89]

Equation 2. The equation for the Flack parameter (x) determines the ratio of enantiomorphic structures (X and $\overline{X}$) and the final structure (C).[89]

$$C = (1\text{-}x)\,X + x\,\overline{X}$$

1.4.3 Stochastic and non-stochastic crystallization

Stochastic processes are those that are probabilistic in nature and involve some level of randomness.[90] But the crystallization of chiral molecules is not always stochastic.[76] Quartz is an example of chiral crystal made up of achiral SiO_2 building blocks. From 1891 to 1973, various researchers collected 10,000 quartz samples from 19 different deposits and concluded that the *d*-quartz and *l*-quartz samples over the surface of Earth are equally

abundant.[78] In 1854, Pasteur stated that for quartz and strontium diformate he obtained a mixture of crystals of both chiralities, where for $MgSO_4$ and $KHSO_4$, he obtained only crystals of one chirality sense.[91] Further examples of non-stochastic crystallization among conglomerate crystallization of achiral molecules are provided in **Table 2**.

Table 2. Conglomerate crystallization of achiral systems displaying non-stochastic results.

Material	Observation	Space group	Reference
Diprotonated tetrakis-(4-sulfonatophenyl) porphyrin ($H_4TPPS_4^{2-}$)	There are 95.6% (+)-aggregate was formed in several hundred independent experiments during ten years investigation.	No crystal structure	[92]
3-(perfluoroethyl)-4,5,6,7-tetrafluoro-1*H*-indazole (CSD code YODJIM)	After repeated sublimation, M helix is preferred. (No enantiomeric excess available)	$P3_2$	[93]
3-(perfluoropropyl)-4,5,6,7-tetrafluoro-1*H*-indazole (CSD code YODJOS)	After repeated sublimation, P helix is preferred. (No enantiomeric excess available)	$P2_12_12_1$	[93]
2-propyl-1*H*-benzimidazole	The sublimation from achiral solution preferentially gives (-)-product.	$P2_12_12_1$	[94]
$[Zn(S_2CNEt_2)_2(vinim)]$ (1; vinim = 1-vinylimidazole	The spontaneous resolution for bulk sample indicated the ee% is approximately 90%.	$P2_1$	[95]
$Co(H_2L)(4,4'\text{-bipy})\cdot H_2O$ [1; H_4L = thiophene-2-phosphonic acid	There are 26 crystals constructed with achiral building blocks that have left-handed helical chain.	$P2_1$	[96]
Coordination polymer $[CuCl_2(H_2O)(caffeine)]_n$	The polymer can form both structures randomly, but preferentially yielded 93% ee% of A-2. 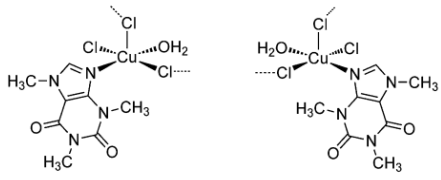 *A-2* *C-2*	$P2_12_12_1$	[97]
Potassium bisulfate	One of the enantiomorph is preferentially formed.	Not reported	[91]
Magnesium sulfate heptahydrate	Pocklington observed 16 crystals out of 22, all of them having the same optical activity.	$P2_12_12_1$	[49, 98]
Potassium bichromate	Right-handed crystals dominantly formed from achiral solution.	P1	[59]

Material	Observation	Space group	Reference
Inclusion compound of β-lactam and 4-oxoazetidine-2-yl benzoate	Varied from 98% ee to 8% ee, depending on the host-guest ratio.	$P2_12_12_1$	[71]
Co-crystal of tri-*o*-thymotide and quaternary ammonium salt	Preferentially crystallized in the (+)-crystal form.	Not reported	[67]

Similar to the distribution of both enantiomorphs of quartz as being equally abundant, Kipping and Pope observed the same stochastic distribution in the crystallization of sodium chlorate crystals (*d*:*l* = 1571:1577) from 46 independent experiments.[4] Of these, 22 experiments had more dextrorotatory sodium chlorate crystals and 23 of the experiments had more levorotatory sodium chlorate crystals.[4] In 1990, Kondepudi reported the stochastic crystallization pattern of sodium chlorate in a static solution can be broken with stirring.[99] Sodium chlorate, like quartz, is another conglomerate forming from an achiral salt, $NaClO_3$. As one of the famous conglomerate examples, scientists proved the crystallization of sodium chlorate randomly formed both levorotatory crystals and dextrorotatory crystals over more than one hundred and fifty years of studies.[4, 9] In the Kondepudi experiment, 1000 crystals in total were collected with a roughly equal distribution between both enantiomorphs. 525 levorotatory crystals and 525 dextrorotatory crystals were collected, and only 8 of 17 experiments obtained slightly more *l*-crystals than *d*-crystals. In contrast, when crystallization was carried out with stirring, homochiral crystallization occurred yielding either levorotatory or dextrorotatory crystals.[99]

1.4.4 Chiral symmetry breaking

Mirror symmetry breaking is when any degree of chirality is observed when a symmetric or racemic state is expected.[100] Primary nucleation, one of the classical nucleation mechanisms, refers to the formation of new crystal nuclei without the influence of pre-existed crystals.[101, 102] In the case of conglomerate crystallization from achiral building blocks, the first chiral crystal formed in solution is a typical chiral symmetry breaking event.

Primary nucleation can be divided into homogeneous primary nucleation or heterogeneous primary nucleation.[101, 102] The prior refers to the primary nucleation that happens without any impurity and the latter involves a foreign interface such as an additive.[103] There are some examples suggesting chiral additives can result in chiral amplification, for example, the mannitol and dulcitol in sodium chlorate or bromate crystallization. Crystallization of $NaClO_3$ with the influence of D-mannitol mainly yielded dextrorotatory crystals from 3 independent experiments (*d*-:*l*- = 1:0, 13:0, 298:0).[104] Heterogeneous primary nucleation with the same additive,

D-mannitol, in the crystallization of sodium bromate yielded the opposite result (*d*-:*l*- = 5:142). This observation is likely related to the fact that crystal structure of sodium chlorate and sodium bromate with the opposite optical activity have the same absolute configuration (**Figure 11**). The crystallizing of sodium chlorate and sodium bromate in D-dulcitol also showed an opposite effect in the preferential chirality among crystal products. Levorotatory sodium chlorate crystals preferentially formed from the solution (*d*-:*l*- = 3:357) with D-dulcitol, whereas with sodium bromate, dextrorotatory crystals formed preferentially(*d*:*l* = 73:0).[104] On the other hand, chiral symmetry breaking in homogenous primary nucleation, nucleation from a slow-nucleating system due to supersaturation, (in the absence of secondary nucleation) is very rare (**Table 2**).[49, 98, 102]

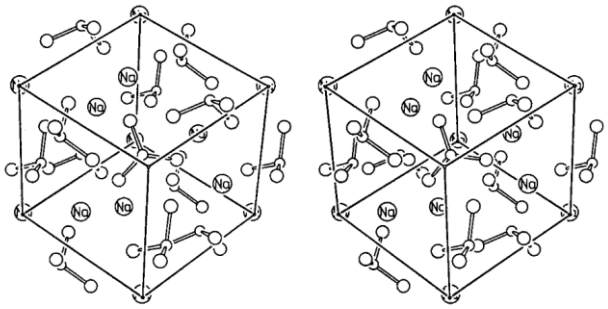

Sodium bromate (space group $P2_13$) Sodium chlorate (space group $P2_13$)

Figure 11. The absolute configuration of sodium chlorate and sodium bromate crystals with opposite optical activity.[105]

1.4.5 Deracemization

Deracemization refers to the process of converting a racemic mixture into a homochiral state.[106] On the other hand, chiral amplification is a process that amplifies any existing chiral imbalance towards a homochiral state. Chiral amplification can be achieved in achiral conglomerate systems under conditions of secondary nucleation, which generates new crystals from pre-existed crystals..[101, 102, 107] Secondary nucleation is often faster than primary nucleation since it can occur at lower levels of supersaturation, which makes chiral amplification possible.[101]

Secondary nucleation can happen with initial breeding, needle breeding, fluid shear, contact nucleation, and more.[102] Initial breeding is introducing seed crystals into the solution.[102] Needle breeding is dendritic-like crystals or needle-like crystals serve as nucleation sites.[102] Fluid shear is the generation of crystals by fluid-induced shear forces exerted on adsorbed molecules moving into existing crystals in solution.[102] Contact nucleation is creating sites for secondary nucleation due to the collision of the preexisted crystal.[102] Experiments

from the Kondepudi lab, McBride lab and Szurgot lab demonstrate experiments where secondary nucleation provide chiral amplification results in conglomerate crystallization (more detail in **Chapter 2**).[2, 99, 107]

Viedma ripening is a deracemization method starting from a racemic mixture that relies on accelerated secondary nucleation.[30] The known mechanism of this chiral amplification is different from the classical nucleation theory but relies on (i) the chiral amnesia effects, (ii) common ancestor effects, and (iii) enantiomer-specific oriented attachment.[108-110] Chiral amnesia is when a homochiral conglomerate crystal dissolves in solution loses its original chirality and has the ability to crystallize into a new crystal of either chirality regardless of the chiral identity of the original crystal.[109] The common ancestor effect is when a crystal is broken down into smaller daughter crystals that all have the same chirality as the mother crystals.[108] Enantiomer-specific oriented attachment is a non-classical nucleation crystal growth process where crystals of the same chirality fuse together in an oriented fashion to form a larger crystal.[111] Viedma ripening also named attrition-enhanced deracemization, can proceed under different conditions, such as grinding, temperature cycling, and solvent cycling.[30-32] The key concept is allowing the chiral species to rapidly change their chirality under non-equilibrium conditions to grow via secondary nucleation and enantiomer-specific oriented attachment. Viedma ripening amplifies tiny chiral imbalances or random chiral fluctuations in racemic mixtures.

In the first report of Viedma ripening, 6 g *d*-sodium chlorate and 6g *l*-sodium chlorate were stirred in 10 mL saturated solution at 200-600 rpm in the presence of grinding media (glass ball: 3 mm of diameter, weight: 2-8 g).[112] During 24 hours of processing, the racemic mixture of sodium chlorate crystals deracemize to either all levorotatory or all dextrorotatory crystals. The time to reach a homochiral state depends on the size of the grinding media and the stirring speed.[112] The process was shorter with smaller grinding media and faster stirring speed. After 24 hours stirring at 600 rpm with 4 g of grinding media, the chirality reached homochirality after 24 hours (**Figure 12**).[112]

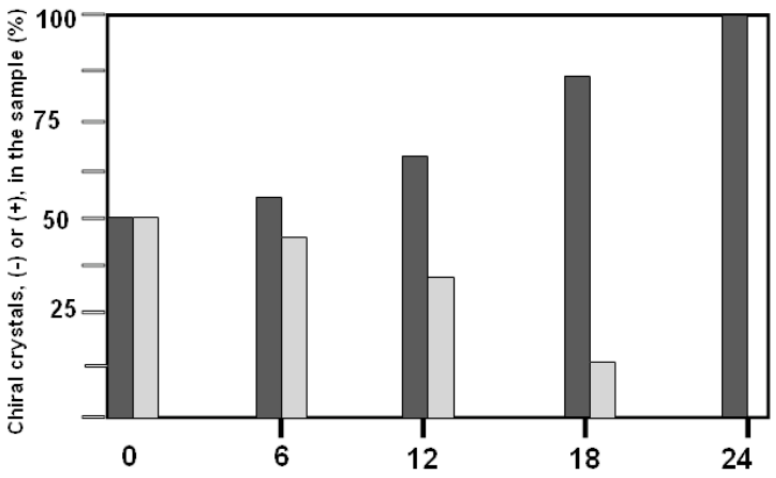

Figure 12. A racemic mixture of sodium chlorate crystals became homochiral after 24 hours of stirring with 4 g grinding media at 600 rpm.[112]

Temperature cycling is another form of Viedma ripening, which can promote deracemization.[113-115] Viedma suggested that the supersaturation gradient caused by the temperature difference in an unstirred system drives the deracemization process. The crystals at the bottom hotter zone are more prone to dissolve while the crystals that move to the top cooler zone by convection are more likely to grow.[30] They assumed the chiral symmetry breaking in each experiment is coming from efficient mixing generated by collapsing bubbles.[30] They obtained 53% cases of homochiral *l*-enantiomorphs and 47% cases of *d*-enantiomorphs from 60 independent experiments of sodium chlorate boiling experiments.[30]

Viedma ripening is not limited to conglomerate system from achiral building blocks. These experiments require racemization in solution to be amplified to homochirality. For example, the atropisomer 1,1'-bi-2-naphthol (**Figure 13**) and its derivatives can racemize under acidic conditions and can undergo complete attrition enhanced deracemization.[116, 117] There are more examples of Viedma ripening of chiral molecules, but this thesis focus on the Viedma ripening of conglomerate crystal systems originating from achiral building blocks.[118-120]

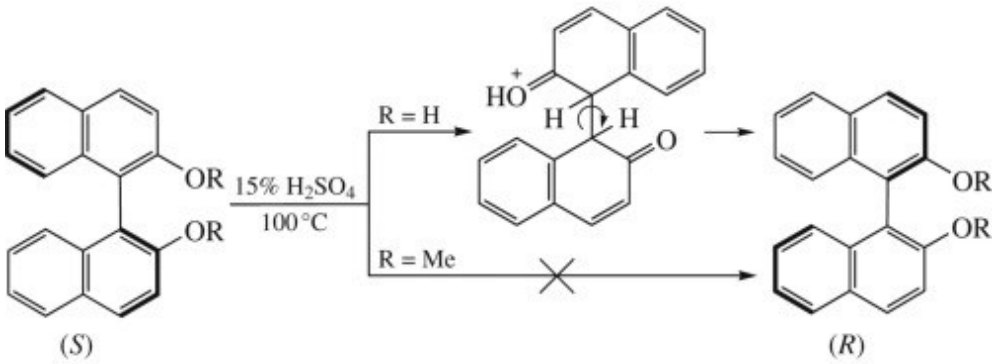

Figure 13. Racemization of 1,1'-bi-2-naphthol under acidic condition.[116]

2 Investigation of Deracemization and Chiral Symmetry Breaking of Conglomerate Crystal with Benzil

2.1 Introduction

Deracemization is a conventional method for obtaining pure chiral material from scalemic or racemic material. Chiral purity is very important for the pharmaceutical industry since chiral material has different biochemical or chemical properties.[109] Viedma ripening, amplifying tiny chiral imbalances in a racemic conglomerate crystal mixture, involves crystals dissolving and reforming under grinding.[112] In the Viedma ripening experiment of conglomerate crystals composed of achiral compounds, like sodium chlorate, loss of chirality upon dissolving, with new crystals forming randomly, eventually leads homochirality. [112]

Viedma ripening is inspired by the research of Kondepudi, who amplified the chirality among racemic conglomerate crystals by promoting secondary nucleation thus minimizing primary nucleation.[121] In Kondepudi's 1990 study, homochiral crystals were obtained through a single mirror symmetry breaking primary nucleation event followed by amplified secondary nucleation once the mother crystal is struck by the rotating stir bar.[99] Szurgot's group explored historical experiments of sodium chlorate crystallizations in 1995, finding that not all stirring experiments resulted in homochiral crystals.[2] They hypothesized that saturation levels might affect outcomes.[2] To test this, they cultivated sodium chlorate crystals in flat-bottomed crystallizers, observing the impact of saturation levels and seed chirality.[2] Eventually, Szurgot's group determined that the saturation level influences this secondary nucleation amplification process. A visualization of the effect of saturation on the chiral outcome in the stirred crystallization of sodium chlorate is shown in **Figure 14**, where ($r = \frac{\#\,(d-crystal)}{\#\,(d-crystal) + \#(l-crystal)}$).[107]

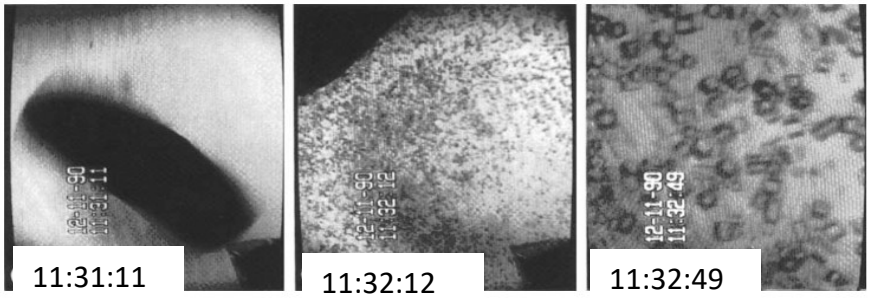

Figure 14. The formation of many daughter crystals one minute and a half after the first mother crystal is struck by the stir bar.[107]

In Viedma's 2011 experiment, the chiral symmetry breaking among 4 samples of hot supersaturated solution (prior to crystallization) was the same. The experimental setup features a 700 mL cylindrical reactor heated with an electric blanket, equipped with a distilling head for solvent removal and a central rod holding four 1.5 mL glass cups, positioned 2.5 cm apart. These cups can be adjusted vertically to sample four regions of the hot supersaturated solution. The solution becomes supersaturated after 70-80 mL of water evaporated after which the four samples were raised above the saturated solution. The solution in the flask and the four sample cups crystallized immediately after sampling and the chirality of the precipitate in the four samples matched the chirality of the crystals from the bulk solution in 14 out of 15 runs. The results suggest that mirror symmetry breaking can occur before visible crystal growth, where the 'mother nuclei' (or chiral pre-nucleus) governs the uniform chirality obtained in all four samples and the bulk solution.

A group from Korea tried to understand why the crystals of sodium chlorate forming on a solution surface tends to share the same chirality.[11] Drops (0.19~2 μL) of sodium chlorate solution were covered with a fluorinated carbon oil (FC-40) on PMMA-coated glass substrates (PMMA: poly(methyl methacrylate)) and dried at constant temperature (30-90℃).[11] Crystal growth and chirality determination were monitored with a polarized light microscope, which revealed dendritic growth.[11] This observation suggested primary nucleation is strongly suppressed and that secondary nucleation by contact occurred.[11] They mentioned that small fluctuations, like microflow, might cause secondary nucleation in the absence of mechanical agitation.[11] Besides, they point out that the possibility to have two or more primary nuclei forming on a small droplet is extremely low.[11] The observation of two similarly sized crystals on one drop suggested that secondary nucleation could start at an early stage immediately after the first nucleus appeared. They do not believe that the saturation level is important in chiral symmetry breaking in small drop evaporation, but rather that the volume of the solution drop is more important.[11]

The experiments above proposed two hypotheses: the first pertains to the mirror symmetry breaking of sodium chlorate due to secondary nucleation leading to chiral amplification, and the second suggests limiting primary nucleation leads to mirror symmetry breaking with subsequent secondary nucleation to amplify chirality. The research described in this chapter explores three experiments to investigate how spontaneous primary nucleation, secondary nucleation, and rapid changes in temperature (supersaturation) can influence the chiral amplification of benzil. According to Maggioni's group who studied the stochastic behavior of primary nucleation of sodium chlorate, small volume experiments are advantageous.[122] Small volume experiments helps to eliminate differences in supersaturation caused by temperature variation.

2.2 Results and Discussion

The exploration of nucleation processes and their impact on enantiomeric excess (ee%) outcomes holds paramount significance in chirality studies. There are two key steps in the chiral amplification of conglomerate systems originating from achiral building blocks: primary and secondary nucleation.

In this research the primary nucleation and secondary nucleation behavior of benzil was investigated in small volume capped PCR tubes. Although some primary nucleation and secondary nucleation experiments of sodium chlorate were recorded in a larger scale setting, smaller scale and more repetitive experiments with benzil provide insight into crystal chirogenesis (*i.e.* origin of chirality) and the relationship between primary and secondary nucleation.[121]

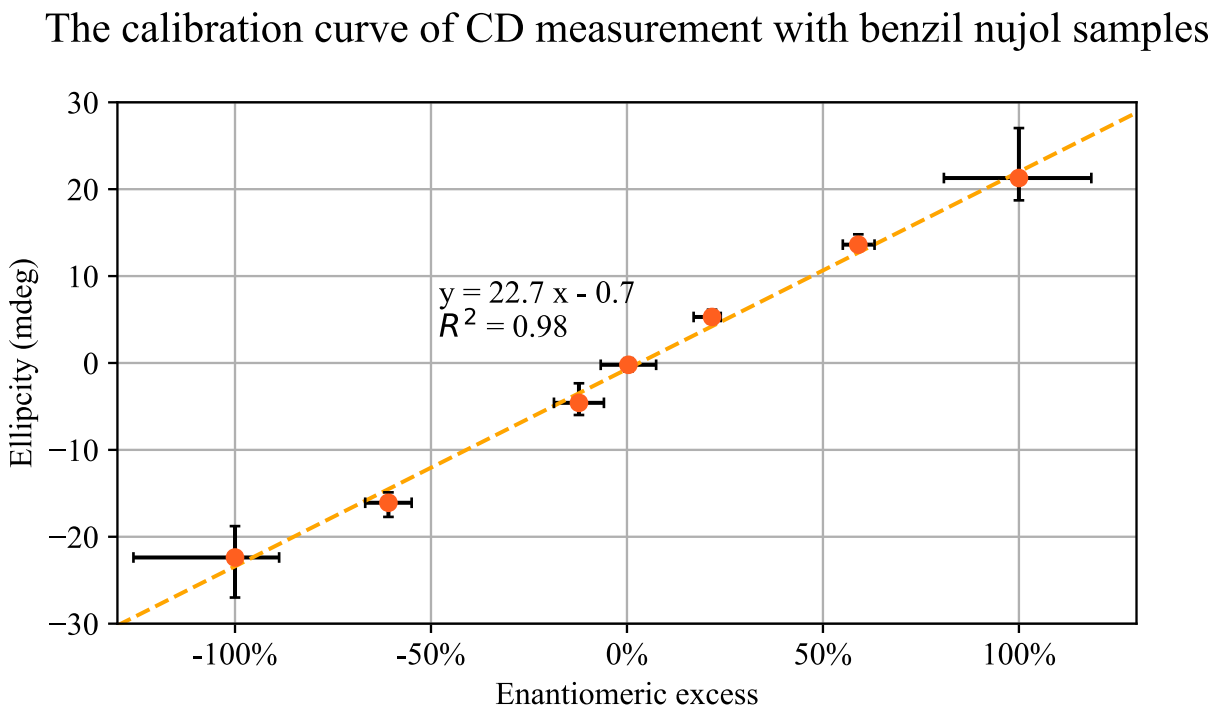

Figure 15. The CEE calibration curve of benzil nujol samples (15 % wt/wt).

There is no report mentioning if benzil crystallizes in a stochastic fashion or not. The commercial sample of benzil solid from our lab has about 26% ee.[123] To confirm if benzil is a suitable material for stochastic crystallization, quick precipitation experiments of benzil were explored. There are 7 experiments repeated with

the same process and measured by CD, which were compared with the calibration curve built using samples of known enantiomeric excess. The measurement of the racemic point (0.34% ee) was obtained from an average measurement of -0.21 mdeg (standard deviation: 0.5, sample number: 9). The CD signal of the quick precipitation samples ranged from -1.0 to 0.4 mdeg) with an average (7 independent experiments) % ee of 2% (independent experiments: 0.7% ee, -0.4% ee, 2.6% ee, 1.1% ee, 5.6% ee, -1.3% ee and 4.4% ee). The enantiomeric excess was estimated based on the calibration curve prepared with known samples (**Figure 15**). It should be noted that the antisolvent method is not a common way of preparing racemic material from achiral conglomerate systems.[103] There are several groups that reported secondary nucleation can occur or even dominate crystallization during antisolvent crystallizing. This was indeed observed during the optimization of this set of experiments.[102, 124, 125] But, all data obtained from the optimized quick precipitation experiments had a value within the range of measurement error, which is the enantiomeric excess range of the same racemic mixture (**Figure 16**).

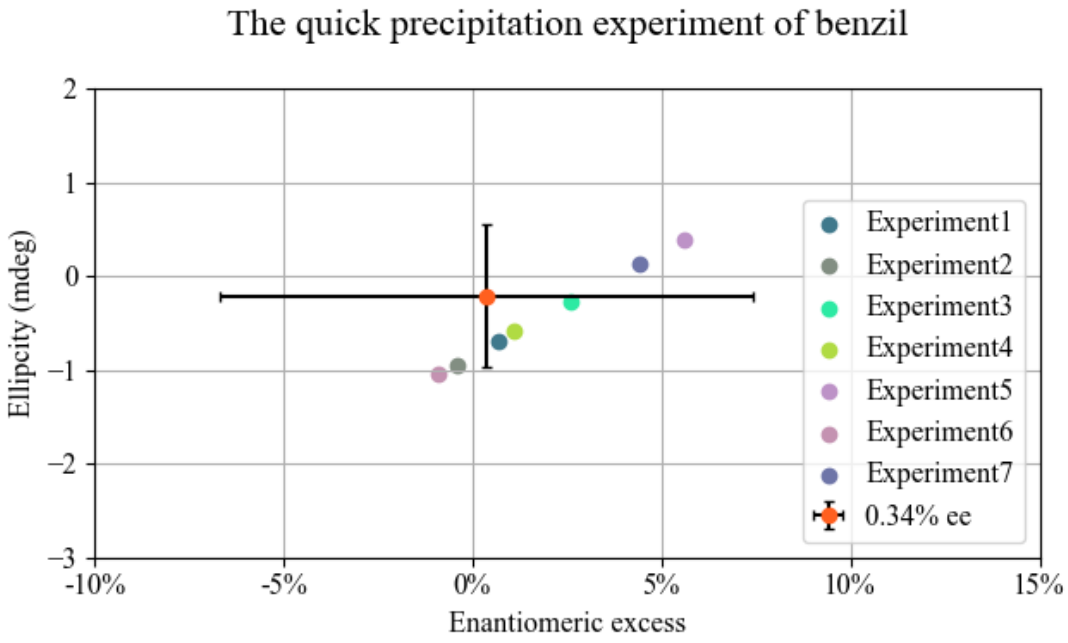

Figure 16. Racemic mixture of benzil solid can be collected from repetitive rapid precipitation experiments.

The expected chiral outcome from cooling the benzil solution from 60℃ to 20℃ is expected to be dominated by primary nucleation.[102] The enantiomeric excess data from 20 experiments distributed around 0% ee (**Figure 17**). According to literature, primary nucleation is highly unpredictable.[122] Although many studies mention that primary nucleation is stochastic, this experiment provides further evidence, indicating the randomness of primary nucleation, especially from the perspective of chiral distribution among the crystal

population. The results are distributed on both the (-) and (+) sides. Clearly chiral amplification from secondary nucleation is also playing a role.

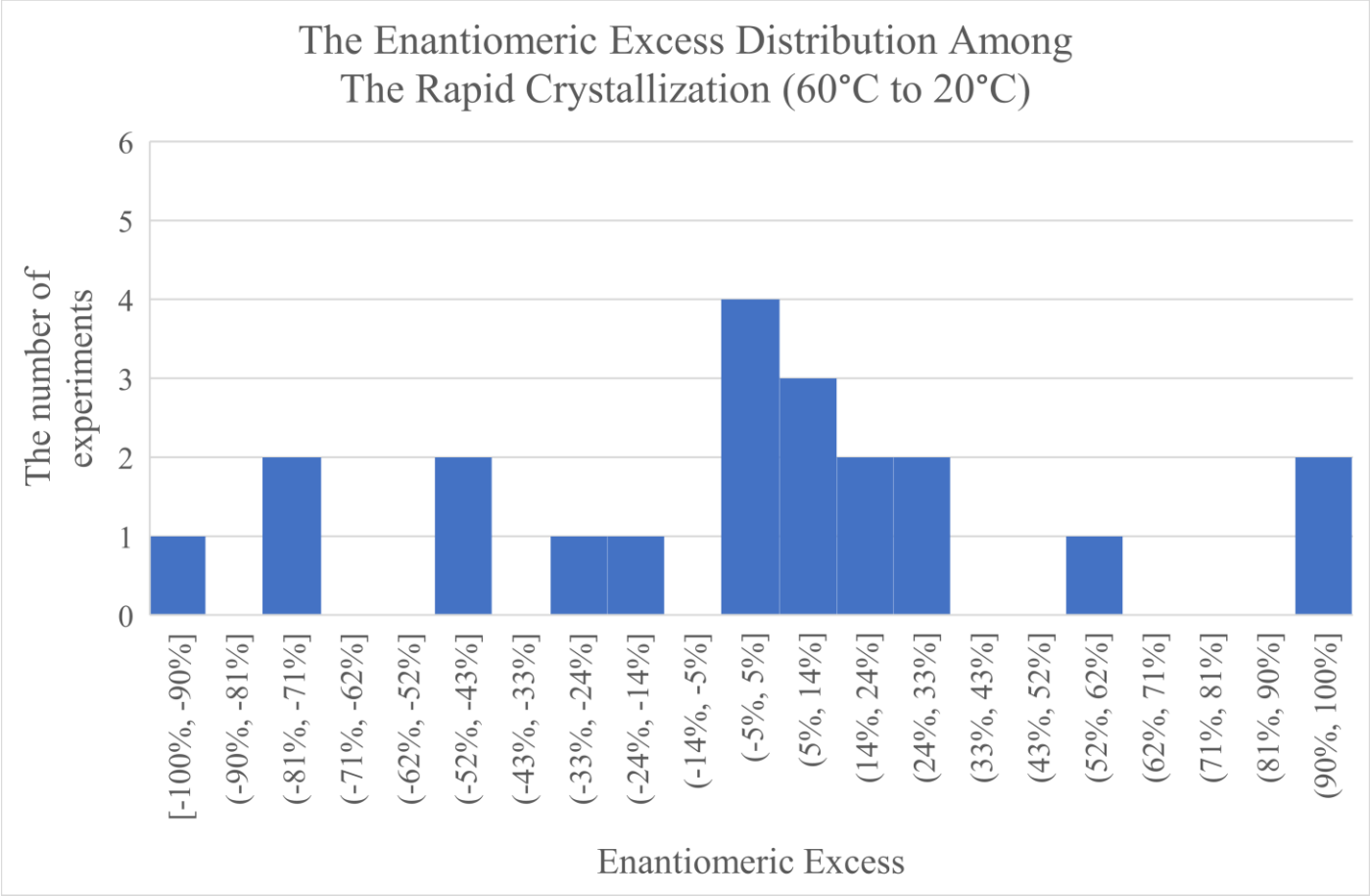

Figure 17. Crystallization of benzil from 60 ℃ to 20 ℃ shows more results close to racemic.

The rapid crystallization of benzil at -78℃ does not show a clear trend towards the racemic or homochiral states among 53 independent experiments. The result from this experimental set shows mainly scalemic mixtures (**Figure 18**). When the solution contacts with the dry ice-isopropanol mixture, dendrite formation (secondary nucleation) happened immediately. The dendrite formation suggested secondary nucleation, however, the distribution of enantiomeric excess does not show the expected bimodal pattern.[11, 102] Instead, the 53 independent experiments were scattered without any obvious central clustering when the temperature decreased from 60℃ to -78℃. There is no strong bias resulting in a negative result or positive result among those experiments. The lack of a clear central tendency suggests the unpredictable nature of crystallization under these conditions. The racemic, homochiral positive, or homochiral negative outcomes appear equally probable.

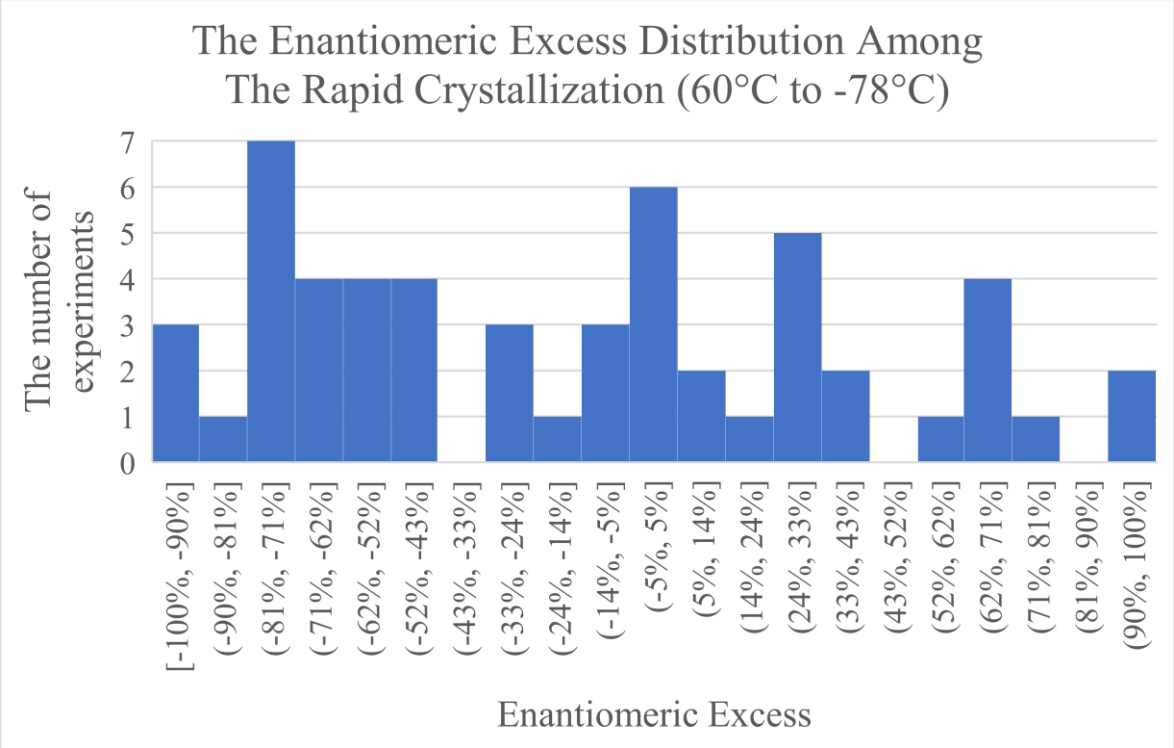

Figure 18. Enantiomeric excess distribution when crystallizing benzil from 60℃ to -78 ℃.

Sonication is a way to introduce crystallization. Whether sonocrystallization is governed by primary nucleation, secondary nucleation, or non-classical nucleation has no solid conclusion yet. Some literature mentions that ultrasound can decrease the metastable zone of crystallization.[103, 125, 126] In the metastable zone, the solution is supersaturated but not saturated enough to spontaneously initiate nucleation. As metastable zones become narrow, nucleation can occur at lower saturation levels.[125, 126] On the other hand, ultrasound generates bubbles in solution, which caused fluid shear as they collapse which may favor secondary nucleation.[127]

The chiral distribution pattern obtained from the rapid crystallization with sonication indicates a bimodal distribution (**Figure 19**). The peaks at the extreme positive and negative ends indicate a bias towards homochirality. Out of 34 experiments, almos half (18 experiments) show high % ee results (ee% ≥80% or ee% ≤-80%). The population distribution is higher at both ends (higher enantiomeric excess) and lower in the middle, with only 2 experiments close to racemic (10% ≥ ee%≥ -10%). These observations suggest low primary nucleation and high secondary nucleation causing significant, yet stochastic, chiral amplification under ultrasound conditions (50/60 Hz).

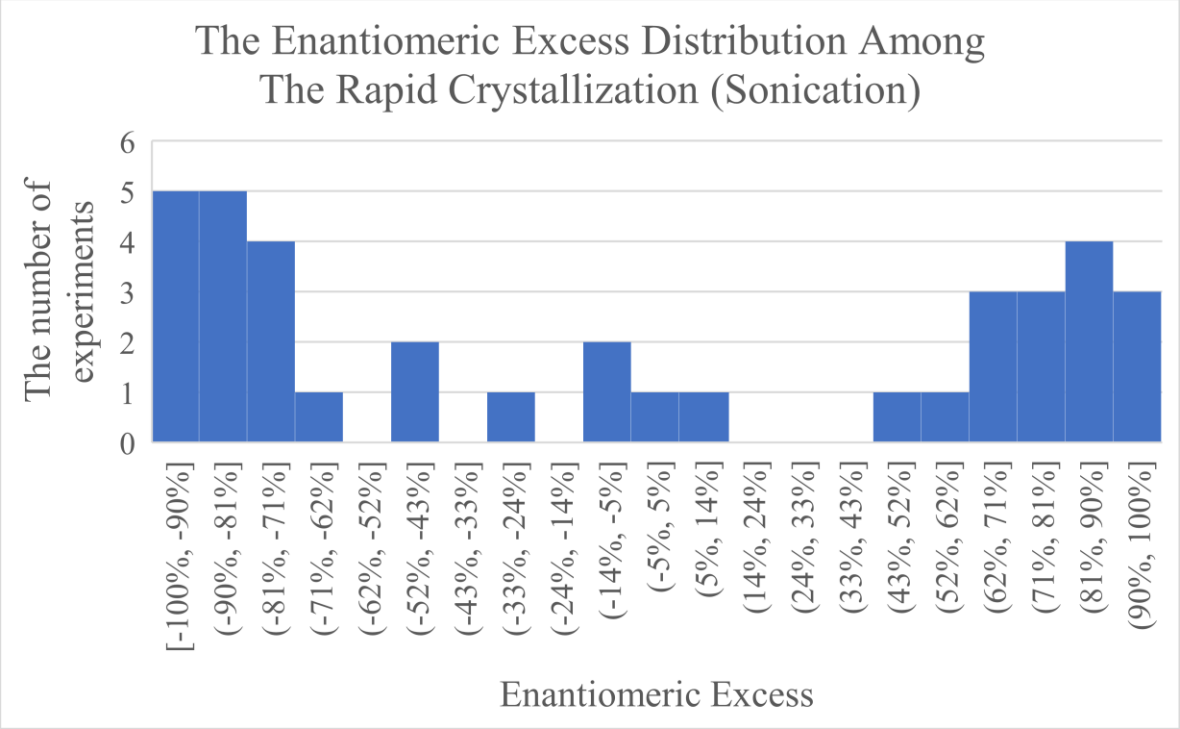

Figure 19. Enantiomeric excess distribution when crystallizing a supersaturated benzil solution under sonication at 50/60 Hz

2.3 Conclusion

In these conglomerate crystallization experiments of benzil, the chiral outcome can be observed under the condition of antisolvent, temperature change, or sonication. It is believed that the observed changes are due to changing the relative degree and speed of primary crystal nucleation versus secondary crystal nucleation.

In the quick precipitation crystallization using large volumes of antisolvent, racemic mixtures of benzil were obtained indicating that there was significant and rapid primary nucleation (stochastic) to overcome the potential for chiral amplification from secondary nucleation. Similarly, when decreasing the temperature from 60℃ to 20℃ stochastic primary nucleation was still observed. With the dendrite formation involved, one form of secondary nucleation, the sample enantiomeric excess became less predictable when temperature decreasing from 60℃ to -78℃. The sonocrystallization experiments displayed a stronger preference for chiral amplification and this could be due to enhanced secondary nucleation as cavitation bubbles collapse.

The first crystal formation, primary nucleation, breaks the chiral symmetry in the conglomerate crystallization of achiral molecules. The chirality of the second crystal generated in the solution can be stochastic or identical to the pre-existing crystal. Chiral amplification leading to high enantiomeric excess can result from secondary nucleation *via* contact nucleation or dendrite formation, for example.[99] Small volume crystallization can be a useful means of studying primary and secondary nucleation by minimizing the effects of temperature gradients in each system. It provides the possibility of observing primary nucleation with a similar setting as secondary nucleation. Solvent loss from the small Eppendorf tubes needs to be monitored and minimized in order to obtain the most reliable results using this method.

Observing the behavior of primary and secondary nucleation is very important for understanding the process of chiral amplification, which leads to scalemic or homochiral material in a controllable way. In the temperature cycling experiment from the Viedma lab and the evaporation experiment of the Bak lab both showed crystals with the same chirality are preferentially formed.

3 Viedma Ripening of Decacyclene

3.1 Introduction

Viedma ripening is a relatively new deracemization technique developed in 2005.[112] This process can amplify tiny chiral imbalances in solid-state conglomerate racemic mixtures to homochirality. Viedma ripening has been demonstrated quite universally towards conglomerate crystals made up of both achiral and chiral building blocks (**Figure 20**).[112, 116-118, 128] Viedma ripening is a non-equilibrium process that relies on achirality or a racemizing agents in solution and the crystal growth and dissolution is driven away from equilibrium through attrition or grinding. The key step for deracemization in Viedma ripening is enantiomer-specific oriented attachment, a non-classical crystal growth mechanism where small chiral crystals of the same chirality fuse together to make a larger crystal rather than dissolve.[12, 111] These larger crystals will be broken down through attrition to increase the population of the dominant chirality until homochirality is reached.[108] The Viedma ripening of benzil and decacyclene is described in this chapter.

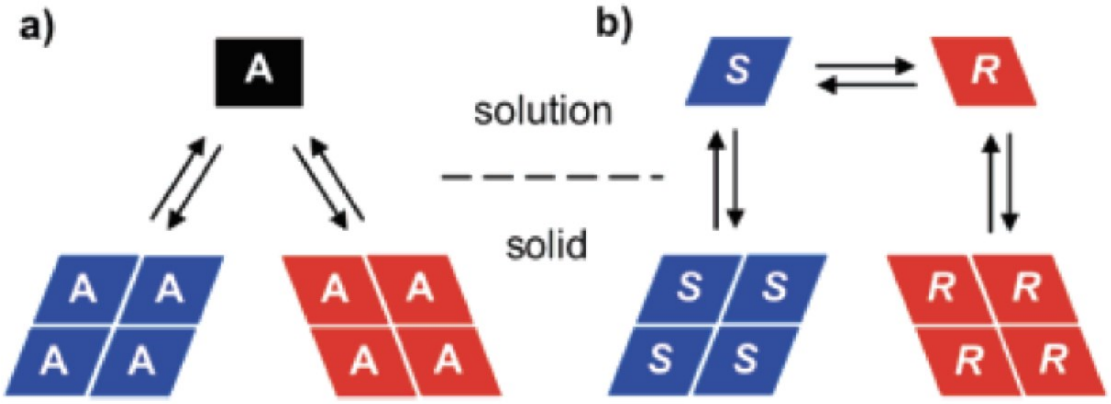

Figure 20. The Viedma ripening process of conglomerate crystal with (a) achiral building blocks and (b) chiral building blocks.[128]

Decacyclene is symmetric, polycyclic aromatic compound forming conglomerate crystals (**Figure 21**).[129] This compound's chirality originates from its propeller conformation due to intramolecular hinderance.[129] This chiral conformation can rapidly change due to the low energy barrier (3 kcal/mol), which allows it to undergo Viedma ripening.[130] Decacyclene crystallizes in the orthorhombic $C222_1$ space group.[129] Interestingly,

conglomerate crystals of decacyclene have an unusual helical twist.[129] With regard to this twist, Pascal *et al.* speculate that, "Since crystallization of decacyclene from solution yields both right- and left-handed helical crystals, it is tantalizing to think that there may be a direct relationship between the macroscopic handedness of the ribbon-like crystals and the absolute configuration of the decacyclene molecule contained within."[129]

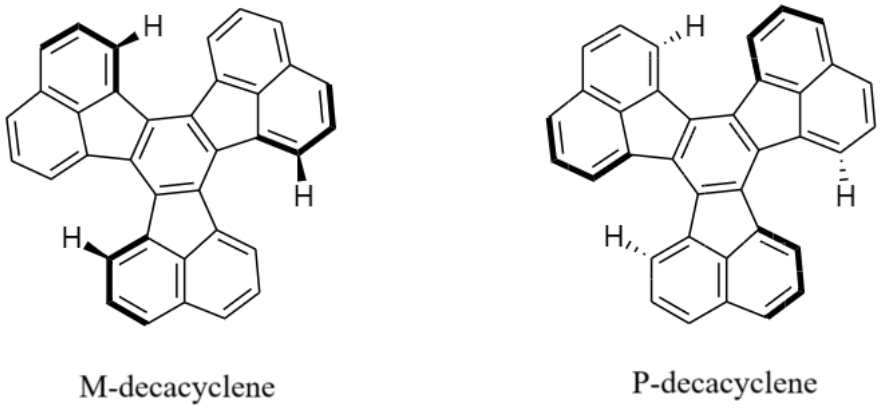

Figure 21. The chiral conformations of decacyclene.

Twisted crystals are crystals that exhibit a helical or twisted morphology. Distinguishing the twist of the crystals is easier compared to finding small differences between two conglomerate crystals. Theoretically speaking, chiral crystals are capable of forming twisted arrangements based on their inner structure, specifically the atomic arrangement and lattice.[131, 132] Twisted arrangements are influenced by factors such as strong intermolecular interactions or lack of centrosymmetry. [131]

3.2 Result and Discussion

There are several materials reported to be successfully amplified through Viedma ripening process. In a paper published in 2016, the Cuccia group reported the deracemization of 10 materials.[111] One common point among all those materials is they are all conglomerate crystals from achiral building blocks. As highlighted throughout this thesis, formation of conglomerate crystals is essential for this amplification process.[30]

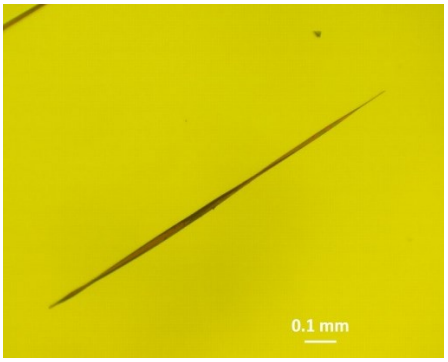

Figure 22. A decacyclene single crystal (P twist) obtained from the slow evaporation of a nitrobenzene solution.

Decacyclene can form conglomerate crystals in helical shape as **Figure 22**. Based on the twisted direction of the crystal, the chirality can be predicted according to the work of a previous student, Munendra Yadav. The circular dichroism (CD) signal of the M crystal with a twisted in counterclockwise had a positive signal, and the crystal twisted in clockwise showed a negative signal in CD measurement (**Figure 23**).

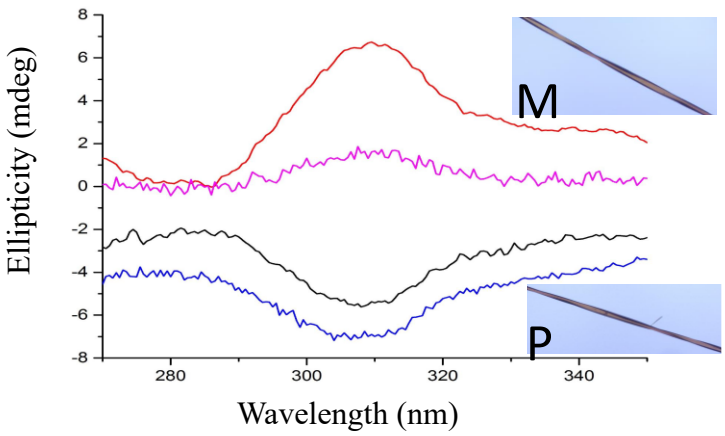

Figure 23. The circular dichroism signal of decacyclene is correlated to the helical twist of the decacyclene crystal. (Contributed by Munendra Yadav)

One of the goals in this project is growing single crystals large enough for CD measurements. However, the size of crystal in **Figure 22** was too small to show a CD signal. To confirm the chirality correlated to the morphology, several different solvent systems were investigated. Preparing crystals with antisolvent vapor slowly diffusing in a good solvent is a possible method for generating large crystals, but in the experiment diffusing acetone and methanol vapor in nitrobenzene system, the crystals were too small for CD analysis (**Figure 24**). The

crystals collected from the crystallization with acetone as the antisolvent vapor were fine and short, on the other hand, the crystals collected from methanol as antisolvent were longer. It may relate to acetone as more volatile compared to methanol. Besides, the concentration of the solvent in this experiment can be lowered as well. A relatively high concentration of the good solvent might result in smaller crystals rather than larger crystals.

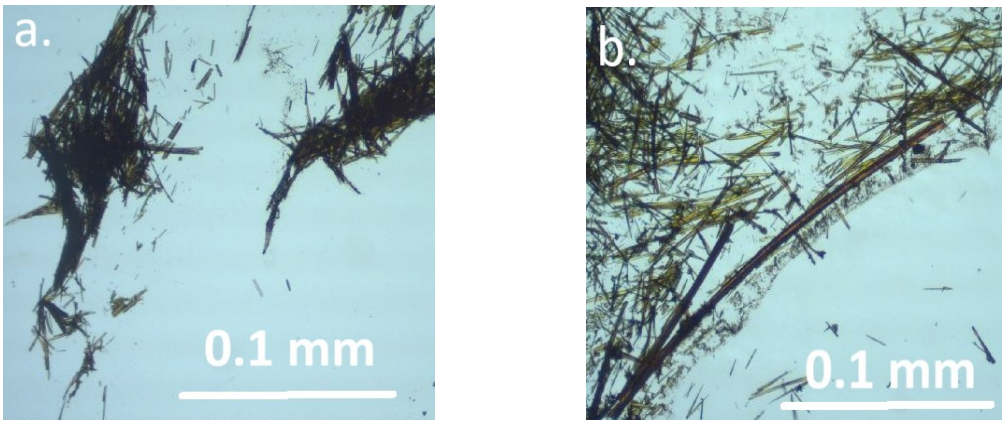

Figure 24. Decacyclene crystals collected from antisolvent system. a) diffusion of acetone in saturated nitrobenzene solution. b) diffusion of methanol in saturated nitrobenzene solution.

Dr. Robert A Pascal mentioned 1,1,2,2,-tetrachloroethane might a better substitute than nitrobenzene, since the crystal would have low helical pitch in flat solvent as nitrobenzene (personal communication)? Should I keep it. However, the crystal can hardly precipitate from the solvent mixture of 1,1,2,2-tetrachloroethane and benzene in a 1:1 ratio after 15 days in the fumehood. On the other hand, the 1,1,2-trichloroethane mixture with benzene in 1:1 ratio seems to give longer crystal and also formed more easily (**Figure 25**).

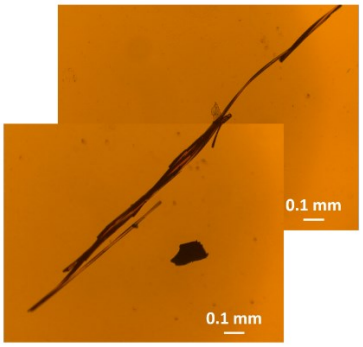

Figure 25. This decacyclene crystal cluster was obtained from the slow evaporation of a 1:1 mixture of 1,1,2-trichloroethane and benzene.

Herein, the chiral amplification of decacyclene using Viedma ripening was demonstrated for the first time. The chiral CD signal stopped increasing 15-21 days after the first amplification signal was observed. Viedma

ripening can amplify both in the CD-positive and CD-negative direction while the speed of amplification can be slower or faster depending on the sample (Figure 24).

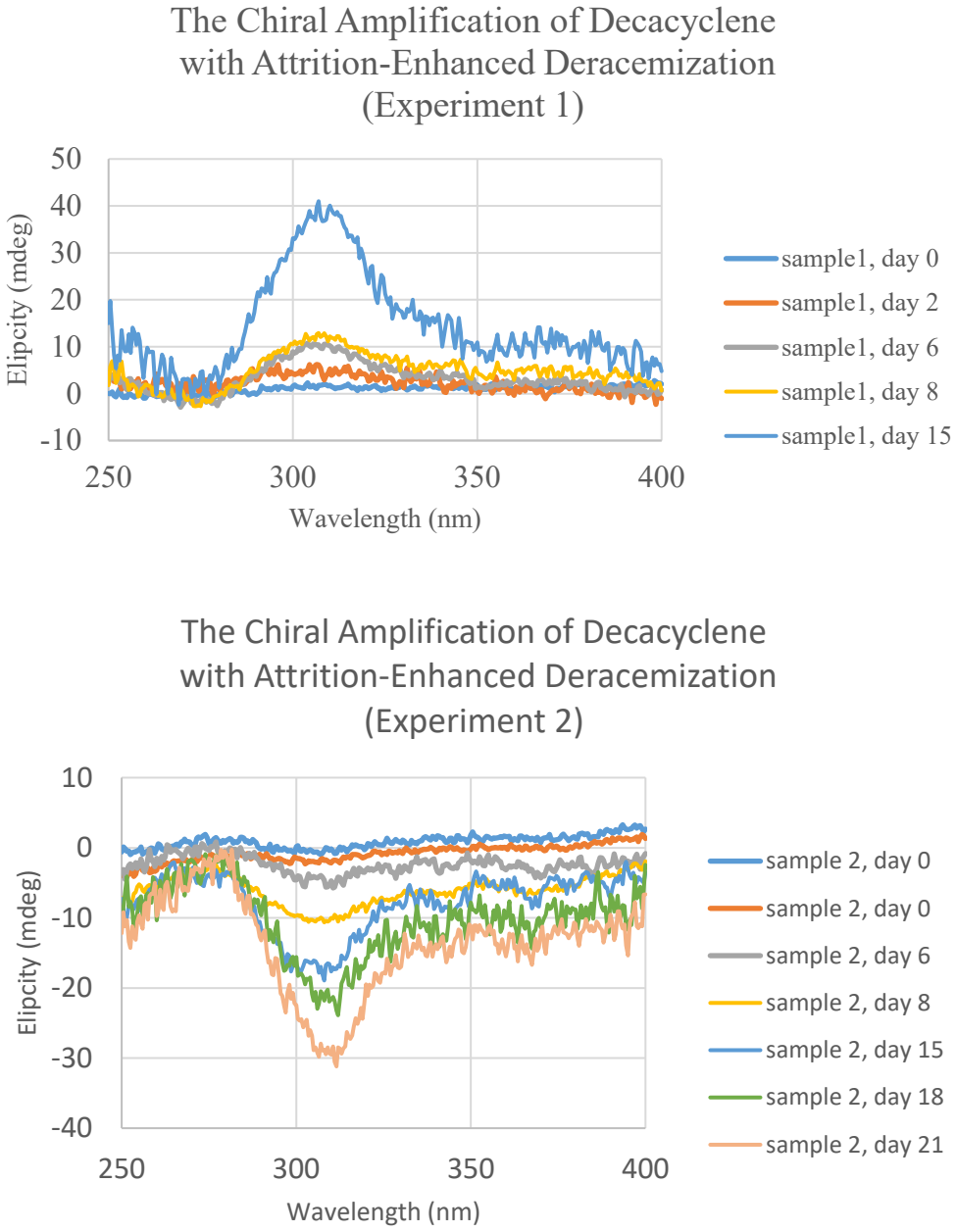

Figure 26. The chiral amplification process of decacyclene during Viedma ripening as visualized using CD

Another material that can successfully process chiral amplification is benzil. The benzil conglomerate crystals in the lab are large enough to provide homochiral material, therefore, it is possible to confirm if the benzil reached a homochiral state. The benzil Viedma ripening takes much less time compared to decacyclene (**Figure**

27). The enantiomeric excess of benzil samples at various times was estimated with the calibration curve prepared as described in **Section 2.2**.

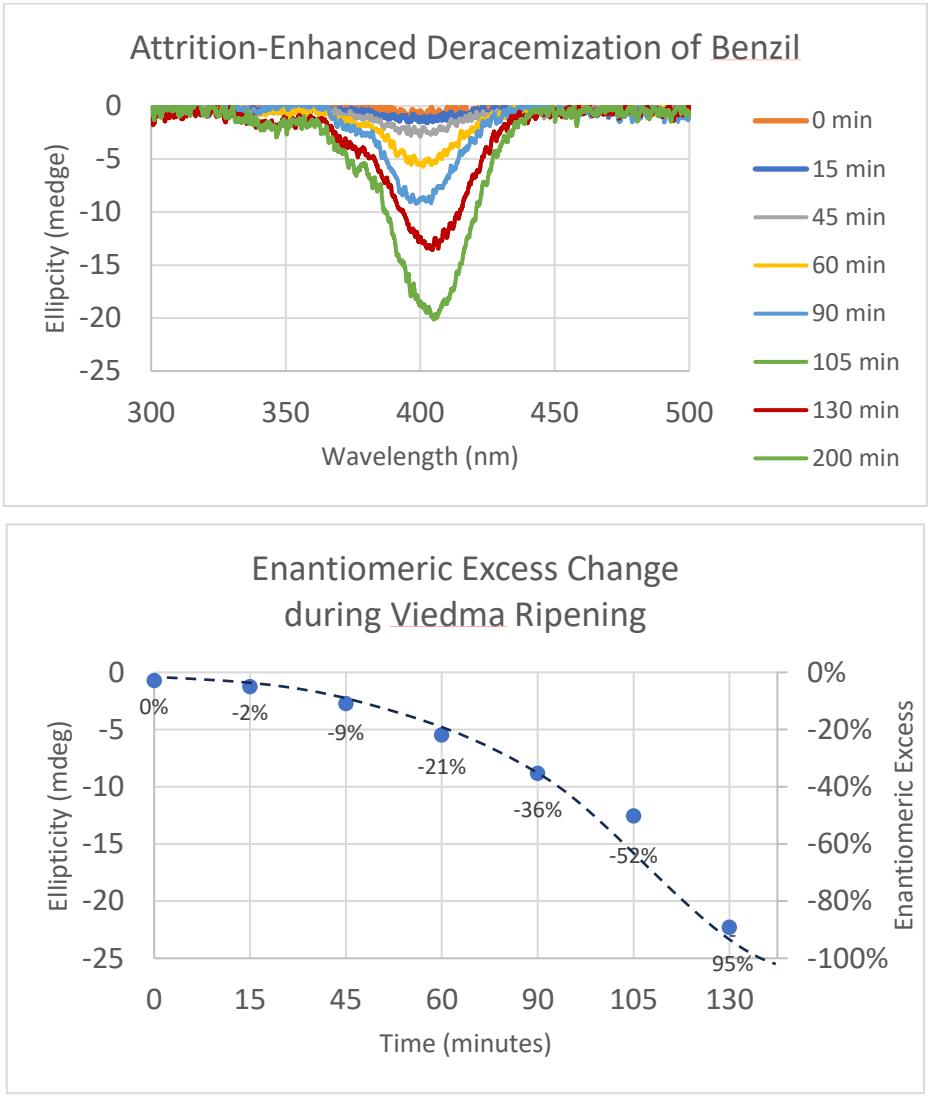

Figure 27. The chiral amplification process of benzil during Viedma ripening as visualized using CD

The enantiomeric excess of benzil samples were estimated with the calibration curve prepared with 15% (wt/wt) benzil nujol samples of known enantiomeric excess. The homochiral powder from single crystals were mixed according to **Equation 1**. Sample with 100%, 59%, 22%, 0%, -12%, -61%, and -100% were prepared for the CD calibration curve measurements (**Section 2.2**).

The Viedma ripening is a relatively new deracemization method which can amplify transient chiral imbalances within racemic mixtures. The low racemization energy barrier of decacyclene allows it to rapidly racemize in solution. It is believed that the slow deracemization of decacyclene (2-3 weeks) is due to its low solubility which would slow down the racemization of decacyclene. Tri-*o*-thymotide is achiral in solution state, but it can form inclusion compound with solvent molecules and adopt chiral conformation as an atropisomer. ToT is a future candidate for testing the chiral amplification of an atropisomer with Viedma ripening.

3.3 Conclusion

For the first time, homochiral conglomerate crystals of decacyclene from a racemic mixture were obtained with Viedma ripening. This process was successfully monitored using circular dichroism spectroscopy as shown in the Figure 26. A racemic mixture of decacyclene crystals was amplified to homochirality after 15 to 21 days of attrition enhanced deracemization. Several crystallization methods were attempted for preparing suitable decacyclene single crystals, yet more exploration is needed.

Benzil is a well-known example of a conglomerate crystal system built up from an achiral molecule. To obtain conglomerate crystals with designed enantiomeric excess, it is necessary to build a corresponding calibration curve from homochiral material mixing at known ratios. The Viedma ripening of benzil confirmed once again that this process can deracemize racemic conglomerate crystals constructed from achiral molecules.

4 Non-Stochastic and Directed Chiral Crystallization of Epsomite

4.1 Introduction

The investigation of epsomite, a mineral renowned as Epsom salt, had been studied since the 19 century.[49, 132] Epsomite captured the attention of scientists as crystallizing into conglomerate crystals from the achiral building blocks: magnesium, sulfate and water.[133] This work reviews the early literature in the field highlighting that epsomite preferentially crystallized into one enantiomorph rather than forming a racemic mixture. The non-stochastic crystallization of epsomite crystal growth was verified in our lab. Furthermore, the influences of chiral additives on the non-stochastic crystallization of epsomite was also investigated. The findings indicate that chiral additives act to break the mirror symmetry and can direct the non-stochastic crystallization towards different outcomes.

Recall that the chirality of the underlying building blocks determines the chirality of the chiral crystal: homochiral molecules always form homochiral crystals of a single chirality.[26, 42, 43] Crystallization of a racemic mixture yields an equal mixture of enantiomers within the crystal's unit cell. In the case of crystallization in one of the Sohncke space groups, it results in an equal mixture of homochiral crystals (*i.e.* conglomerate crystallization).[26, 42, 43] When chiral crystals are constructed from achiral building blocks, crystallization normally shows no preference for one enantiomorph over the other. However, conglomerate crystallization from achiral building blocks allows for manipulating factors that could change the chiral outcome, biasing one chiral crystal form over the other. In this context, the impact of D-asparagine and L-asparagine on the CEE of the non-stochastic crystallization of epsomite is notable.

Early research on chiral crystals often relied on optical activity and hemihedral face analysis.[27] In 1904, Dufet highlighted distinct morphological differences between the two enantiomorphs of epsomite (**Figure 28**).[98, 134] More examples of conglomerate systems that can be resolved manually by Pasteurian resolution (*i.e.* triage) are provided in **Table 1** (**Chapter 1 section 1.4.2**).

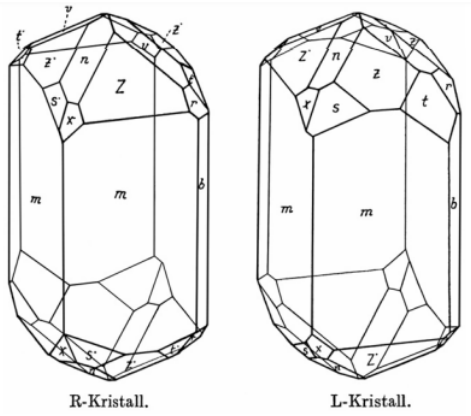

Figure 28. Right and left handed epsomite crystals grown without additive.[134]

Later, researchers observed changes in morphology in the crystallization of epsomite with borax (sodium tetraborate, $Na_2B_4O_5(OH)_4 \bullet 8H_2O$) as an additive. Borax highlights the asymmetric morphology of epsomite, making the *b* face more prominent, as illustrated in **Figure 29**.[134] Further investigations revealed borax's selective adsorption on the 111} and $\overline{1}\overline{1}\overline{1}$} faces of epsomite, which significantly influences the growth rates of these crystal faces.[135, 136] Such directional growth amplified the visibility of hemihedrism and its relationship with other faces of the crystal.[135-137]

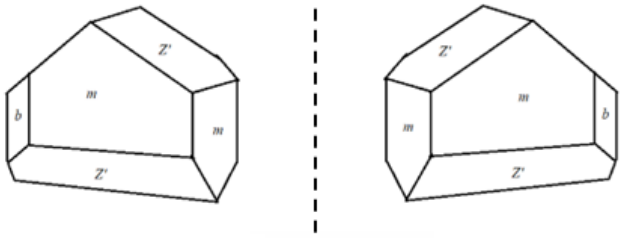

Figure 29. The morphology of left- and right-handed epsomite crystals grown in the presence of borax, the left crystal displays the *b* faces on the left side of the pair of sphenoids while the right crystal displays the *b* faces on the right.[134]

In Dufet's 1904 paper, he remarked that, of three epsomite crystals with sufficient morphology to identify chirality, they all exhibited identical optical activity (-26°/cm). These three crystals all had the morphology of the left-handed crystal shown in **Figure 29**.[49] However, in 1906, Pocklington grew 22 epsomite crystals, 16 of which displayed sufficient morphology to identify chirality. Remarkably, in this case all 16 epsomite crystals displayed positive optical activity.[98] Based on this observation, Pocklington suggested that the epsomite crystals biased

toward one specific handedness was not a random effect and proposed that the observed symmetry breaking in epsomite crystallization might be related to chiral impurities.[98] It should be noted that many conglomerate crystallizations display a stochastic distribution of enantiomorphs as is the case with sodium chlorate (**Section 1.4.3**).[4, 99] However, Pocklington's hypothesis retains its relevance in this and other conglomerate systems. The crystallization of sodium chlorate and bromate respond to chiral additives resulting in non-stochastic crystallization (**Section 1.4.4**).

There are more examples of chiral symmetry breaking due to the presence of chiral additives during conglomerate crystallization. For instance, L-malic acid monohydrate preferential crystallized from D/L-malic acid in the presence of L-asparagine.[138] The chiral polymeric additive, L-poly(N^6-methacryloyl-L-lysine) (PMAL) directs a chiral bias result in the conglomerate crystallization of racemic threonine (90% ee D-threonine) racemic allo-threonine (90% ee D-allo-threonine) and racemic aspartic acid (> 90% ee D-aspartic acid).[12] Directed symmetry breaking of ethylenediammonium sulfate (EDS) crystals using chiral amino acids was investigated in the Cuccia group where they showed that: (i) for 13 amino acids the addition of the D-isomer directed the chiral symmetry breaking towards homochiral *dextrorotatory* EDS crystals whereas the addition of the L-isomer directed the process towards homochiral levorotatory EDS crystals; (ii) for three amino acids, the addition of the D-isomer directed the chiral symmetry breaking process towards homochiral levorotatory EDS crystals while the addition of the L-isomer directed the chiral symmetry breaking towards homochiral dextrorotatory EDS crystals, and (iii) for three amino acids, the presence of D- or L-amino acids showed no directing effect.[139]

4.2 Results and Discussion

The resolution of epsomite is linked to its crystal morphology according to the literature.[49] Since epsomite is not isotropic, it's two optical axes complicate determining optical activity using polarized optical microscopy or polarimetry.[134] Additionally, magnesium sulfate lacks a chromophore required for generating a circular dichroism signal.[86] However, given the presence of heavy atoms in epsomite (Mg and S), further chiral analysis using the single crystal x-ray diffraction (scXRD) is possible. Prof. Scott Bohle collected diffraction data from fragments of left-handed and right-handed epsomite crystals and solved their absolute structures using Flack parameter analysis (**Section 1.4.2**) The absolute configuration of left-handed epsomite is shown in **Figure 30**.

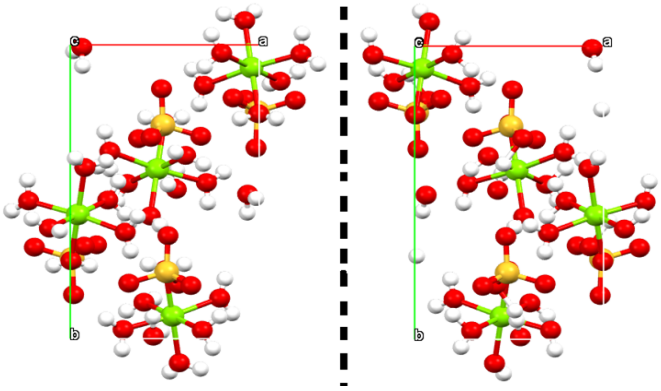

Left-handed crystal Right-handed crystal

Figure 30. The absolute configuration of left-handed and right-handed epsomite crystals.

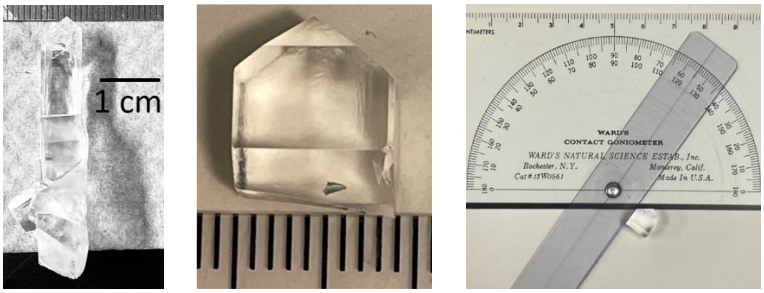

(a) (b) (c)

Figure 31. The crystal morphologies of left- (a) and right-handed (b) epsomite crystals. Interfacial angles measured using a contact goniometer (c).

Data derived from the Flack parameter in the scXRD measurements highlight that the left-handed (x = 0.07) and right-handed (x = 0.02) crystals are distinctly homochiral. The Miller index relates faces of a crystal to a 3-dimensional coordinate system.[85] The interfacial angles of a crystal are related to the elements of symmetry of atoms in the same geometrical arrangement and can be measured using a contact goniometer (**Figure 31**).[85] **Figure 32** shows enantiomorphic crystal models of epsomite built with VESTA (version 3 - a three-dimensional visualization system for crystallographic studies). Measured interfacial angles were compared with the calculated angles derived from VESTA (right-handed crystals:

Table 3 to **Table 7**; left-handed crystals: from **Table 8** to **Table 12**).[85] Although the shape or the size of different faces on a crystal are variable, depending on crystal growth conditions, the angular relation of faces is constant in all crystals with the same makeup.[85]

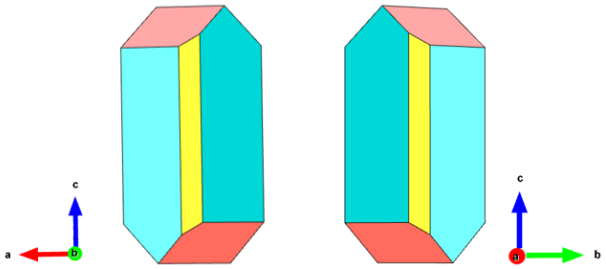

Left-handed Epsomite Right-handed Epsomite

Figure 32. The crystal morphologies of left- and right-handed epsomite crystals built using VESTA (version 3).

Table 3. The interfacial angles of the (100) and ($\bar{1}$00) faces with other adjacent faces in right-handed epsomite crystals.

	Face		Theoretical (°)	Measured (°)	
				Crystal 1	Crystal 2
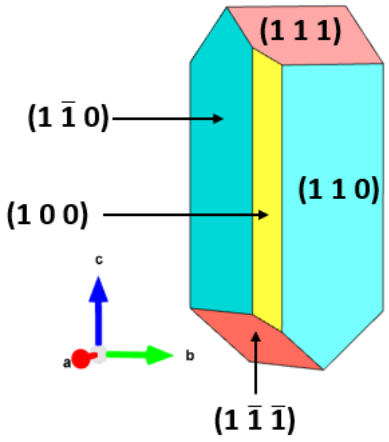	(1 0 0)	(1 $\bar{1}$ 0)	44.97	42	40
		(1 1 1)	63.33	58	60
		(1 1 0)	44.97	44	46
		(1 $\bar{1}$ $\bar{1}$)	63.33	64	63
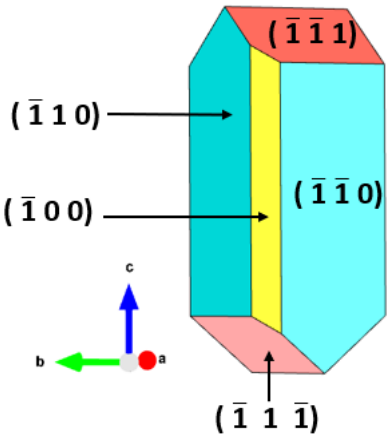	($\bar{1}$ 0 0)	($\bar{1}$ $\bar{1}$ 1)	63.63	64	62
		($\bar{1}$ 1 0)	44.97	45	44
		($\bar{1}$ $\bar{1}$ 0)	44.97	45	44
		($\bar{1}$ 1 $\bar{1}$)	63.33	64	63

Table 4. The interfacial angles of the (111) face with other adjacent faces in right-handed epsomite crystals.

	Face		Theoretical (°)	Measured (°)	
				Crystal 1	Crystal 2
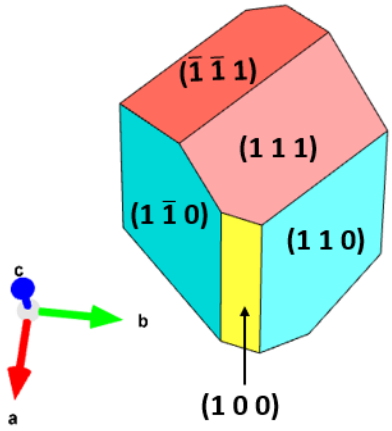	(1 1 1)	(1 1̄ 0)	89.97	90	90
		(1 0 0)	63.63	58	60
		(1 1 0)	51.12	51	52
		(1̄ 1̄ 1)	77.77	78	76
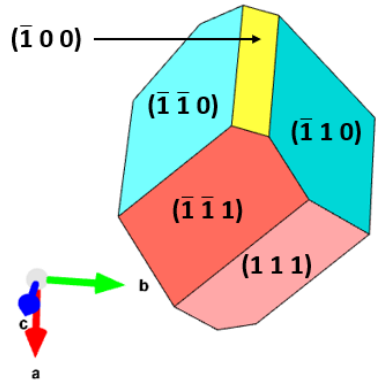	(1 1 1)	(1̄ 1̄ 1)	77.77	78	76
		(1̄ 1̄ 0)			
		(1̄ 0 0)			
		(1̄ 1 0)	90.03	89	90

Table 5. The interfacial angles of the $(1\bar{1}\bar{1})$ face with other adjacent faces in right-handed epsomite crystals.

	Face		Theoretical (°)	Measured (°)	
				Crystal 1	Crystal 2
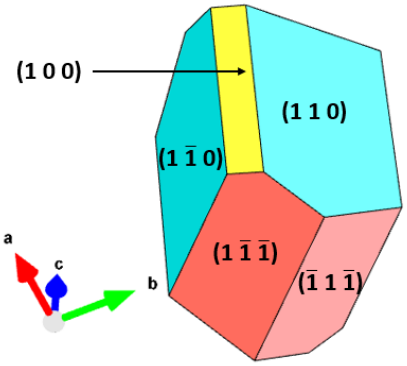	(1 $\bar{1}$ $\bar{1}$)	(1 $\bar{1}$ 0)	51.11	52	52
		(1 0 0)	63.63	64	62
		(1 1 0)	89.96	89	87
		($\bar{1}$ 1 $\bar{1}$)	77.77	82	80
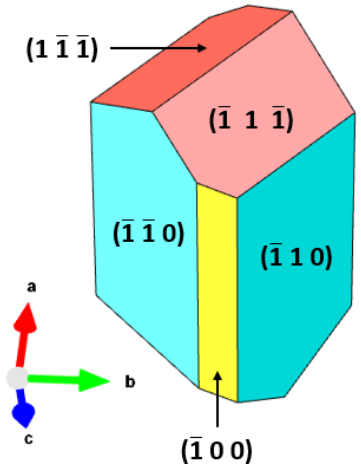	(1 $\bar{1}$ $\bar{1}$)	($\bar{1}$ 1 $\bar{1}$)	77.77	82	80
		($\bar{1}$ $\bar{1}$ 0)	90.03	90	90
		($\bar{1}$ 0 0)			
		($\bar{1}$ 1 0)			

Table 6. The interfacial angles of the $(\bar{1}1\bar{1})$ face with other adjacent faces in right-handed epsomite crystals.

	Face		Theoretical (°)	Measured (°)	
				Crystal 1	Crystal 2
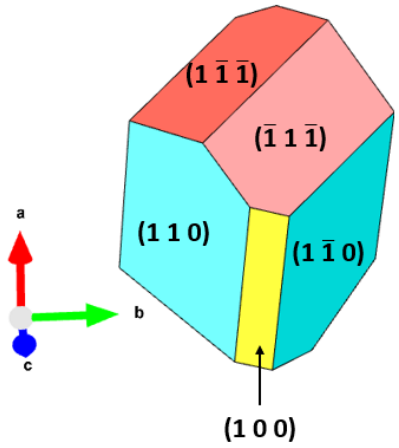	($\bar{1}$ 1 $\bar{1}$)	(1 $\bar{1}$ 0)			
		(1 0 0)			
		(1 1 0)	90.03	90	90
		(1 $\bar{1}$ $\bar{1}$)	77.77	82	80
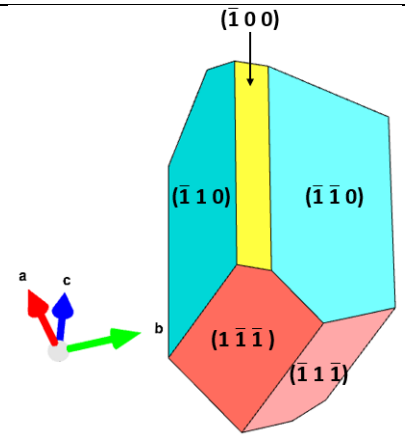	($\bar{1}$ 1 $\bar{1}$)	(1 $\bar{1}$ $\bar{1}$)	77.77	82	80
		($\bar{1}$ $\bar{1}$ 0)	89.97	90	90
		($\bar{1}$ 0 0)	63.63	64	63
		($\bar{1}$ 1 0)	51.12	50	50

Table 7. The interfacial angles of the $(\bar{1}\bar{1}1)$ face with other adjacent faces in right-handed epsomite crystals.

	Face		Theoretical (°)	Measured (°)	
				Crystal 1	Crystal 2
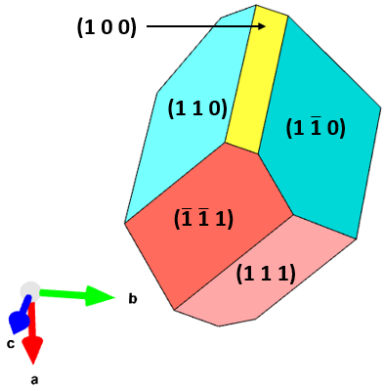	($\bar{1}$ $\bar{1}$ 1)	(1 $\bar{1}$ 0)	90.03	90	90
		(1 0 0)	63.63	64	62
		(1 1 0)	51.12	51	50
		(1 1 1)	77.77	78	76
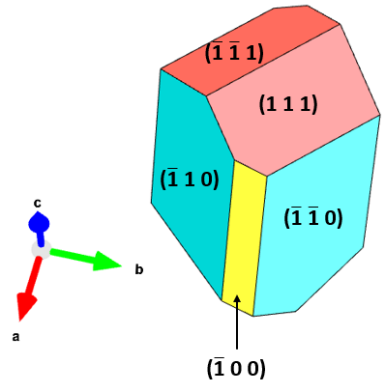	($\bar{1}$ $\bar{1}$ 1)	(1 1 1)	77.77	78	76
		($\bar{1}$ $\bar{1}$ 0)			
		($\bar{1}$ 0 0)			
		($\bar{1}$ 1 0)	89.97	90	90

Table 8. The interfacial angles of the $(0\bar{1}0)$ and (010) faces with other adjacent faces in left-handed epsomite crystals.

	Face		Theoretical (°)	Measured (°)	
				Crystal 1	Crystal 2
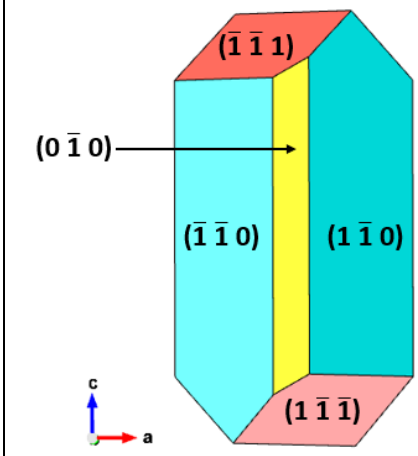	(0 $\bar{1}$ 0)	(1 $\bar{1}$ 0)	45.03	42	42
		($\bar{1}$ $\bar{1}$ 1)	90.03	90	92
		($\bar{1}$ $\bar{1}$ 0)	45.03	46	46
		(1 $\bar{1}$ $\bar{1}$)	63.66	60	60
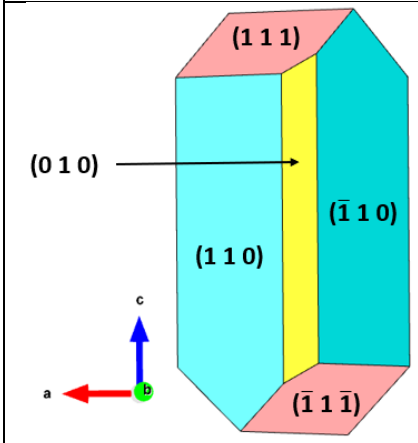	(0 1 0)	(1 1 1)	90.03	90	92
		($\bar{1}$ 1 0)	45.03	46	46
		(1 1 0)	45.03	46	46
		($\bar{1}$ 1 $\bar{1}$)	63.66	60	60

Table 9. The interfacial angles of the $(\bar{1}\bar{1}1)$ face with other adjacent faces in left-handed epsomite crystals.

	Face		Theoretical (°)	Measured (°)	
				Crystal 1	Crystal 2
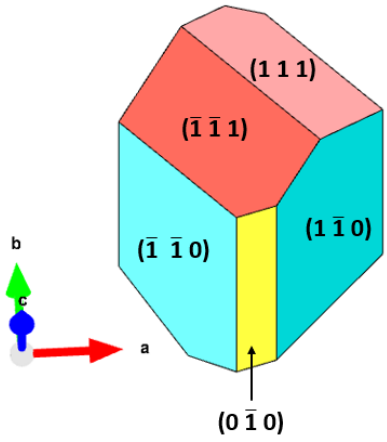	$(\bar{1}\,\bar{1}\,1)$	$(1\,\bar{1}\,0)$	90.03	90	88
		$(0\,\bar{1}\,0)$	90.03	90	92
		$(\bar{1}\,\bar{1}\,0)$	51.12	50	52
		$(1\,1\,1)$	77.77	76	78
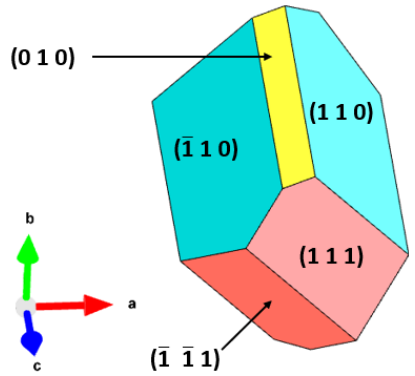	$(\bar{1}\,\bar{1}\,1)$	$(\bar{1}\,1\,0)$	89.97	86	86
		$(0\,1\,0)$			
		$(1\,1\,0)$			
		$(1\,1\,1)$	77.77	76	78

Table 10. The interfacial angles of the $(1\bar{1}\bar{1})$ face with other adjacent faces in left-handed epsomite crystals.

	Face		Theoretical (°)	Measured (°)	
				Crystal 1	Crystal 2
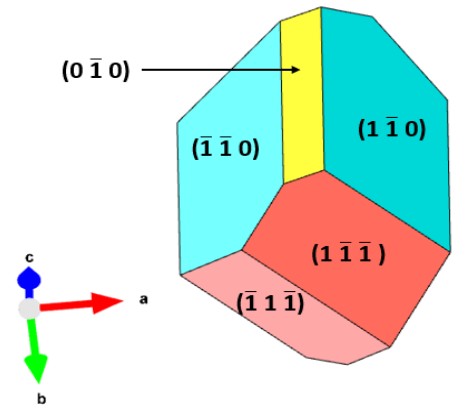	$(1\bar{1}\bar{1})$	$(1\bar{1}0)$	51.11	50	52
		$(0\bar{1}0)$	63.66	63	64
		$(\bar{1}\bar{1}0)$	90.03	88	90
		$(\bar{1}1\bar{1})$	77.77	76	78
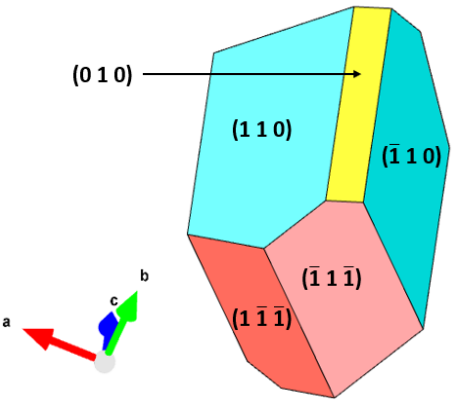	$(1\bar{1}\bar{1})$	$(\bar{1}10)$			
		(010)			
		(110)	89.97	88	90
		$(\bar{1}1\bar{1})$	77.77	76	78

Table 11. The interfacial angles of the (111) face with other adjacent faces in left-handed epsomite crystals.

	Face		Theoretical (°)	Measured (°)	
				Crystal 1	Crystal 2
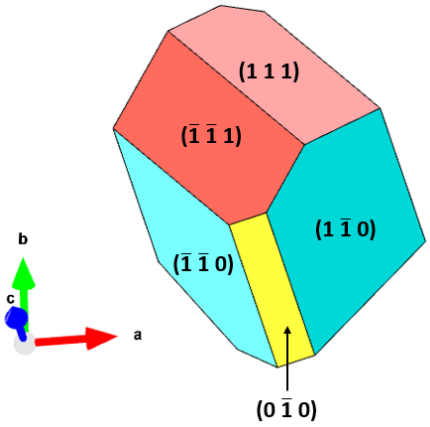	(1 1 1)	(1 1̄ 0)	89.97	86	89
		(0 1̄ 0)			
		(1̄ 1̄ 0)			
		(1̄ 1̄ 1)	77.77	80	80
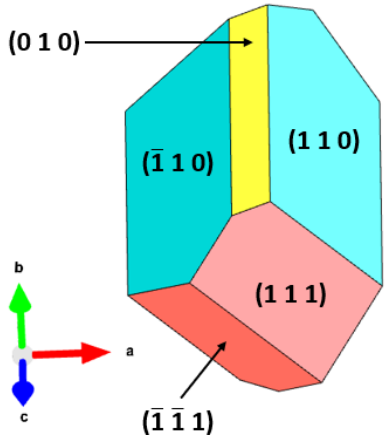	(1 1 1)	(1̄ 1 0)	90.03	90	92
		(0 1 0)	90.03	90	92
		(1 1 0)	51.12	51	50
		(1̄ 1̄ 1)	77.77	76	78

Table 12. The interfacial angles of the ($\bar{1}1\bar{1}$) face with other adjacent faces in left-handed epsomite crystals.

	Face		Theoretical (°)	Measured (°)	
				Crystal 1	Crystal 2
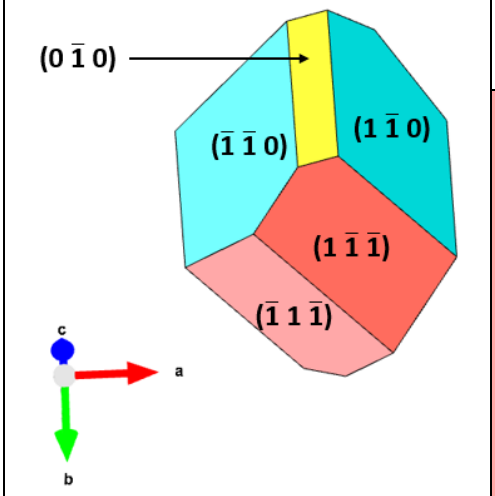	($\bar{1}$ 1 $\bar{1}$)	(1 $\bar{1}$ $\bar{1}$)	77.77	76	78
		($\bar{1}$ $\bar{1}$ 0)	89.97	88	90
		(0 $\bar{1}$ 0)			
		(1 $\bar{1}$ 0)			
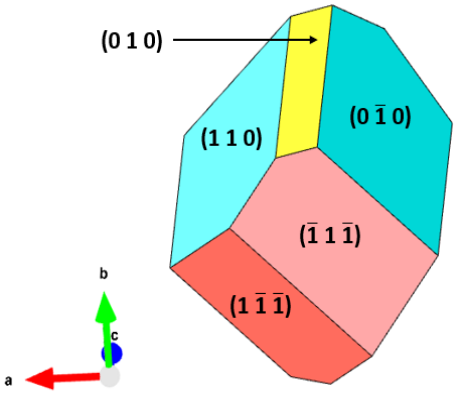	($\bar{1}$ 1 $\bar{1}$)	($\bar{1}$ 1 0)	51.12	50	50
		(0 1 0)	63.66	60	60
		(1 1 0)	90.03	88	90
		(1 $\bar{1}$ $\bar{1}$)	77.77	76	78

After confirming the absolute configuration of epsomite, we have confidence on the chiral identity of each enantiomorph of epsomite crystals. The next step was to investigate the non-stochastic behavior of epsomite crystallization. Dufet reported the crystallization of 3 left-handed crystals.[49] In 1906, Pocklington reported the crystallization of 22 epsomite crystals, where 16 crystals were right-handed and the chirality of the remaining 6 crystals was unable to be determined.[98] In 1966, Belyustin and Rogacheva reported the crystallization of 165 right-handed epsomite crystals and 557 left-handed epsomite crystals.[140] In our study, 139 crystals with sufficient morphology to determine crystal chirality were grown where 134 were right-handed and only 5 were left-handed. The likelihood of epsomite crystallization producing a random outcome is just one out of a million tests, as determined by "the t-test: paired two samples for means", using the number of enantiomorphs from each separate experiment (more information about the analysis; **Section 8.1**). Epsomite is a very particular case which tends to form one enantiomorph rather than the other in all reported cases (**Table 13**). In various labs, one of the enantiomorphs consistently dominates in epsomite crystallization, however, the preferred enantiomorph can vary by lab. As seen in the Pocklington and Cuccia Labs, where there's a crystal enantiomeric excess (CEE) of over 90% favouring right-handed crystals.[98] Conversely, Dufet's report and the research of Belyustin and Rogacheva indicated a preference for left-handed enantiomorphs.[49, 140]

Table 13. The summary of crystallization of epsomite crystals without chiral additive.

Source	The Count of Right-Handed Crystals	The Count of Left-Handed Crystals	Crystal Enantiomeric Excess (CEE)
Dufet[49]	0	3	-100%
Pocklington[98]	16	0	100%
Belyustin and Rogacheva[140]	165	557	-54%
Cuccia Lab	134	5	93%
$CEE = \frac{\#\,(right\text{-}handed\ crystal) - \#\,(left\text{-}handed\ crystal)}{\#\,(right\text{-}handed\ crystal) + \#\,(left\text{-}handed\ crystal)}$			

The likelihood of epsomite crystallization being stochastic was only 1% with 60 mM D-asparagine and 2% with 60 mM L-asparagine, as the CEE dropped from 93% (no chiral additive) to 71% and 68%, respectively

(**Table 14**). The influence of the chiral additive became more pronounced with increasing concentration of chiral additive. At a concentration of 0.18 M for both D- and L-asparagine, the chiral outcomes deviate significantly as compared to the chiral outcome in the absence of chiral additive. Specifically, epsomite crystallization with 0.18 M D-asparagine yielded 37 left-handed crystals, which is 7 times more than the left-handed crystals collected from the experiments without chiral additive. This results in a CEE of -28%. In stark contrast, an overwhelming 93% CEE was observed when only borax was present. In the mixture containing 0.18 M D-asparagine, the number of experiments with more left-handed crystals was 11 and the number of experiments with more right-handed crystals was 12. This parity suggests that at such an additive concentration, stochastic epsomite crystallization becomes a tangible possibility, as reflected by the increased probability of 36% with 0.18 M of D-asparagine additive (**Table 14**).

Table 14. The summary of the crystal handedness of epsomite between the pairs of chiral additives at different concentrations

Chiral Additive	**The Count of Right-Handed Crystals**	**The Count of Left-Handed Crystals**	**Crystal Enantiomeric Excess (CEE)**
-	134	5	93%
L-asparagine (0.06 M)	30	5	71%
D-asparagine (0.06 M)	21	4	68%
L-asparagine (0.18 M)	99	22	64%
D-asparagine (0.18 M)	21	37	-28%
If CEE is above 0%, right-handed crystals dominate in this batch of crystals collected.			
If CEE is below 0%, left-handed crystals dominate in this batch of crystals collected.			

Besides, the dominant crystals obtained in each independent experiment is presented in **Table 15** (more details in **Section 8.1**). This observation provides evidence that the dominant species in each compared group with different chiral additives or the concentration of chiral additive is not a random result. The effect of chiral additive 0.18 M D-asparagine and L-asparagine is statistically significantly different from borax, and the lower concentration of asparagine (0.06 M D-asparagine or L-asparagine).

Table 15. The tendency of dominant crystal population of epsomite between the pair of chiral additives

Chiral additive	The Count of Independent Experiments			The total of independent experiments	The ratio of right-handed dominated experiment
	CEE > 0	CEE < 0	CEE= 0		
-	45	0	0	45	100%
L-asparagine (0.06 M)	8	0	0	8	100%
D-asparagine (0.06 M)	4	0	0	4	100%
L-asparagine (0.18 M)	37	4	3	44	84%
D-asparagine (0.18 M)	11	12	2	25	44%
if CEE is above 0%, right-handed crystal is dominant species in this batch of crystal collection					
if CEE is below 0%, left-handed crystal is dominant species in this batch of crystal collection					

The exploration of epsomite's unique characteristics not only contributes to the understanding of chirality in conglomerate crystallization but also has implications for the concept of "disappearing polymorphs." The problem of disappearing polymorphs caused a significant impact in various fields, where the crystal structure of a compound can directly affect properties such as solubility, chemical or physical stability, and bioavailability.[141] There are cases of crystallization where it becomes difficult to obtain a previously known polymorphic form once a new polymorph emerges. It is generally believed that disappearing polymorphs are due to cryptoseeding of the new, more stable, polymorph. The left- and right-handed crystalline forms of epsomite can be considered as mirror-image polymorphs. Why is one chiral form dominantly during crystallization?[49, 98, 142] Herein, we believe the reason is due to a cryptochiral environment as proposed by Pocklington almost 120 years ago! The understanding of why epsomite prefer specific enantiomorphs during the crystallization can potentially offer insights into the underlying mechanisms of polymorphism.

4.3 Conclusion

Epsomite crystallization shows chiral preference in individual experiments as reported by Dufet, Pocklington, and Belyustin & Rogacheva.[49, 98, 140] All epsomite crystallization in our lab favoured the right-handed

enantiomorph. However, a preference for left-handed crystals was observed when epsomite was grown in the presence of D-asparagine (0.18 M), The hypothesis that a cryptochiral impurity in the environment directs the non-stochastic crystallization of epsomite is likely.

5 Conclusion

This project comprised three parts: 1) the investigation of chiral symmetry breaking and chiral amplification of benzil under different conditions, 2) the chiral amplification of racemic mixture of benzil crystals *via* Viedma ripening (*i.e.* attrition enhanced deracemization) and 3) exploring the non-stochastic chiral crystallization and directed mirror symmetry breaking of epsomite. The focus of this research is based on conglomerate crystallization, a process of spontaneously forming homochiral crystals from achiral or racemic building blocks.[15] Conglomerate crystallization can provide insight into mirror symmetry breaking and chiral amplification and deracemization leading to chiral imbalances and homochirality. Understanding mirror symmetry breaking, chiral amplification and deracemization provide a tools and insight for obtaining homochiral materials in a controllable way, which is one of great challenge in Chemistry & Biochemistry.[109]

Primary nucleation is one form of chiral symmetry breaking in conglomerate crystallization from achiral building blocks, since the first crystal formed from an achiral solution breaks the balance between the two chiral forms. The later crystals generated under the influence of existing crystals is known as secondary nucleation. Since the activation energy of primary nucleation is higher than that of secondary nucleation, conglomerate systems are biased towards chiral amplification if secondary nucleation dominates over primary nucleation.[101] This phenomenon was beautifully demonstrated and visualized by the groups of Kondepudi and McBride with complete chiral amplification of sodium chlorate under stirring conditions.[2, 99, 107] On the other hand, Viedma observed the sodium chlorate crystals sharing the same handiness appeared simultaneously.[143] While the group of Bak also observed that the second crystals forming were likely to have the same chirality as the first crystal formed in the same small drop of a sodium chlorate solution,[11, 121] This observation of mirror symmetry breaking asks a question: whether the homochiral result credit to the chiral amplification during secondary nucleation after the primary nucleation, or is there is a 'mother nuclei' in the solution that initiates mirror symmetry breaking?

The first part of the research designed an experiment set up for observing the behavior of primary nucleation and secondary nucleation during the conglomerate crystallization process of achiral molecules. The experiments suggested both primary and secondary nucleation involved in the benzil crystallization experiments under different conditions. There are temperature conditions of driving small volume crystallization that influenced the chirogenesis of conglomerate crystallization from achiral building blocks. All experimental conditions gave results suggesting both primary and secondary nucleation occurred during this process. It was also observed that secondary nucleation had a dominant effect on crystal chirality under sonocrystallization conditions.

Viedma ripening is a deracemization process acting on conglomerate crystals. A solid-state CD calibration curve of benzil chirality was successfully prepared and used to monitor the attrition-enhanced deracemization of benzil. Decacyclene crystalizes as a conglomerate that rapidly racemizes in solution but has a fixed propeller chiral conformation in the solid state. This solid-state chirality of decacyclene was successfully amplified after stirring with grinding media for several days. The slow deracemization process is believed to be due to decacyclene's poor solubility in nitrobenzene which slows down the overall degree of chiral interconversion in solution, a key step in Viedma ripening. Due to the challenges of obtaining large single crystals of decacyclene, more investigations are required in order to confirm the relationship between CD signal and single crystal twist sense. A future project related to deracemization would will be the Viedma ripening of tri-*o*-thymotide another symmetric molecule that adopts a propeller shape in the solid state as a clathrate with certain solvents molecules such as benzene and chloroform.[24] In this case, T*o*T is an atropisomer so that chiral amplification can be investigated in solution.

The last part of this thesis relates to the chiral symmetry breaking of epsomite crystallization. Epsomite is a special case among conglomerate crystalline materials, as it crystallizes in a non-stochastic fashion. For example, epsomite crystals in our lab were grown where most crystals were right-handed (134 of 139 crystals) and only 5 left-handed crystals were obtained. A chiral additive, asparagine, was introduced during epsomite crystallization to observe the directing effect on the resulting chirality of epsomite crystals. In this case the chirality of epsomite crystallization became more racemic in the presence of D-asparagine at 0.18 M. This experiment suggests that chiral additive has a directing effect in non-stochastic crystallization process, and concentration is playing an important role as well.

Overall speaking, this project studied the chiral symmetry breaking behavior of conglomerate crystallization under different conditions. Conglomerate crystallization can lead to chirality amplification. Chirality is essential in various fields, including pharmaceuticals and agrochemicals. Different enantiomers of a chiral drug molecule can exhibit vastly different effects in the human body due to their interaction with chiral biological systems. Therefore, being able to selectively crystallize a specific enantiomer through conglomerate crystallization is essential for producing pharmaceutical compounds with the desired therapeutic properties. Understanding mirror symmetry breaking on conglomerate systems built up from achiral building blocks can shed light on crystal polymorphism, where solid-state chirality may play a role in pharmacokinetics (the study of how drugs are absorbed, distributed, metabolized, and excreted by the body) of pharmaceutical compounds! The processes described herein can help in understanding the fundamental principles of solid-state chirality and

molecular interactions. Researchers can gain insights into how different molecular conformations lead to preferential crystallization of specific chiral conformations. This work also contributes to the field of crystal engineering, where researchers design and manipulate crystal structures for specific applications. This has the potential to yield new materials with tailored solid-state chiral properties.

6 Experimental

6.1 Materials

Benzil (diphenylethanedione, ([CAS 134-81-6], $C_6H_5COCOC_6H_5$, F.W. 210.23 g/mol; 98%), acetone ([CAS 67-64-1, CH_3COCH_3, F.W. 58.08 g/mol; ≥99.5%), nitrobenzene ([CAS 98-95-3, $C_6H_5NO_2$, F.W. 123.11 g/mol; 99%), 1,1,2-trichloroethane ([CAS 79-00-5, $CH_2ClCHCl_2$, F.W. 133.40 g/mol; 97%), 1,1,2,2-tetrachloroethane ([CAS 79-34-5, $CHCl_2CHCl_2$, F.W. 167.85 g/mol; ≥98%), methanol ([CAS 67-56-1, CH_3OH, F.W. 32.04 g/mol; ≥99.8%), benzene ([CAS 71-43-2, C_6H_6, F.W. 78.11 g/mol; ≥99.0%), D-asparagine ([CAS 2058-58-4], $H_2NCOCH_2CH(NH_2)CO_2H$, F.W. 132.12 g/mol; ≥99%), L-asparagine ([CAS 2058-58-4], $H_2NCOCH_2CH(NH_2)CO_2H$, F.W. 132.12 g/mol; ≥99%) were purchased from Sigma Aldrich. Decacyclene ([CAS 191-48-0], $C_{36}H_{18}$, F.W. 450.5 g/mol; 98%) was purchased from GTI Laboratory Supplies. Epsomite ([CAS 10034-99-8] $MgSO_4 \cdot 7H_2O$) was purchased from RW Consumer Products Ltd. (Natural Epsom Salts, Pure Standard Products®) and Laboratoire Atlas Inc. (Epsom Salt, Personnelle®). Borax ([CAS 1303-96-4], $B_4O_7Na_2.10H_2O$, F.W. 381.4 g/mol) was obtained from the Mule 20 Team® brand with 99% purity. Nujol mineral oil ([CAS 8012- 95-1] was obtained from Plough Inc. Potassium bromide ([CAS 7758-02-3]; KBr; F.W. 119.00 g/mol) was purchased from Sigma Aldrich.

6.2 Instrumentation

Solid-state enantiomeric excess was measured with Jasco J-710 circular dichroism spectrometer, which was set with 0.5 nm data pitch, 1.0 nm band width, 1 sec response, standard sensitivity, 100 nm/min scanning speed, 3 times accumulation at room temperature (*ca.* 22 ℃). The scanning range setting The KBr pallet prepared with EVACUABLE PELLET PRESS FOR 13 MM PELLETS.

A home-built magnetic stirrer based on a PINE 101 industrial drive (coupled with a PINE MSRX speed control or Chemglass Life Science® Digital Heating Magnetic Stirrer) was used for Viedma deracemization. Ceramic beads (0.5 mm dia.) were used as the grinding media for Viedma deracemization. Vesta (version 3) software was used to model and index the prominent faces of crystals.

The samples in milliliter scale crystallization were prepared in a sealed PCR tube (PROGENE ®, CAT. #87-200-F) in a thermal cycler (Eppendorf, Mastercycler® personal) regulating temperature between 4 and 99℃ at a rate of 3℃ per second. The temperature of the PCR tubes can be maintained not just from the heat block but also by a heat source in the cover of the thermal cycler, which minimizes the saturation difference generated by

the uneven heat source. The bath sonicator was an Elma Ultrasonic T310, with *ca.* 35 W effective ultrasonic power (frequency: 50/60 Hz).

6.3 Experimental operations

6.3.1 Benzil crystallization in antisolvent (quick precipitation method)

The solution was prepared with 1 g of benzil dissolved in 15 mL of acetone. The benzil acetone solution was slowly added dropwise from a separatory funnel to 500 mL of deionized ice water. The water was constantly stirred with a magnetic stir bar. Stirring allowed the precipitate to disperse evenly without clustering locally. Failure to stir properly can result in zones of enantiomeric excess since the formed solid layer can inhibit contact between the solvent and non-solvent. This can be prevented by stirring (or by lowering the concentration of the benzil solution). Solid benzil was recovered by vacuum filtration and the yield was always above 80%. The enantiomeric excess of benzil solid formed using this method is typically very low (± 5% ee). The optimized conditions described above were obtained after screening many conditions including: the temperature of the non-solvent, the concentration of the benzil solution, the conditions with or without stirring and the mixing method between solvent and non-solvent.

6.3.2 Solubility measurement

In a 20 mL vial with stir bar (PTFE magnetic stirring rod, ring shape, diameter: 7 mm, length 25 mm), the specified amount of solid was added with 10 mL of solvent according to the literature. The vial containing solid, and solvent was capped and placed on a hot plate with stir function for 30 minutes. Repetitive experiments are necessary for confirming the solubility.

6.3.3 Benzil crystallization in PCR tube

The samples were prepared in a sealed PCR tube (PROGENE ®, CAT. #87-200-F) with *ca.* 40 mg benzil and 20 μL acetone, the enantiomeric excess of the starting material was between ± 5%. The tubes were initially heated at 60℃ for 10 minutes to ensure full dissolution. Finally, the sample was rapidly cooled to 20℃ in the thermal cycler and maintained at this temperature for 60 minutes. In one group of crystallization experiments, the temperature was decreased from 60℃ to 22℃, and the other group decreased to -78℃ in a dry ice-isopropanol mixture.[144] The benzil saturation systems take about 12 seconds in each sample to fully crystallize after this cooling process. The final group of samples took advantage of the supersaturated samples that did not crystallize after cooling to 20℃. These samples were sonicated for 2-4 minutes until the supersaturated benzil solution crystallized at room temperature (*ca.* 22℃).

6.3.4 Decacyclene crystallization by antisolvent vapor diffusion

In the crystallization by antisolvent vapor diffusion, the solution was prepared with 0.1 g decacyclene solid in 4 mL nitrobenzene. The decacyclene solution was transferred into a small vial until it reached the 1 mL mark, then transferred into a 20 mL vial with tweezers. The 20 mL vial was capped after adding about 5 mL of antisolvent while the small vial remained open.

6.3.5 Circular dichroism

The measurement of circular dichroism was done with sample diluted with nujol mull or KBr solid. The wavelength setting depends on the material can range from 250-600 nm depending on the material. The data pitch is 0.5 nm. Band width is 1.0 nm. Response took 1 sec. The sensitivity is standard. The scanning speed is range can be 50 to 100 nm/min as needed. Usually, the measurement needs to scan for 3 times at temperature: room temperature *ca.* 22 ℃. The sample prepared in nujol was ground in mortal with certain amount of nujol. The nujol mixture should have a evenly mixture grinded agate mortar and pestle. About 0.09-0.10 g of the benzil/nujol mixture was transferred to the center of a 2 mm thick quartz plate (diameter: 2 cm) and pressed carefully with another quartz plate of the same size. The two quartz plates were gently pressed together to remove bubbles in the sample before placing the sample in the sample holder of the Jasco J-710 circular dichroism spectrometer.

The KBr sample was prepared with oven dried sample mixed with the dried potassium bromide (3 days at 120 C) to make a 70 mg KBr pellet. The solid was grinded with agate mortar and pestle until became fine powder. The 13-mm diameter pellet contained pressed with 5-ton of pressure under vacuum. The sample was measured in the circular dichroism spectrometer, Jasco J-710.

6.3.6 The calibration curve for enantiomeric excess estimation

The sample with known enantiomeric excess were prepared with the powder of single crystals with different chirality. The conglomerate crystals into fine powder with agate mortar and pestle and mixed according to **Equation 1**. The calibration curve presents the CD signal corresponding to the sample with known excess, therefore, the CD signal of unknown sample prepared with the same method as the standard can be plotted in the calibration curve for estimating the enantiomeric excess.

6.3.7 The preparation of racemic material

Some of the commercial materials are racemic, it is not required to prepare another racemic mixture. The chirality of the starting material was measured before the experiment. Materials with single crystal can be

distinguished by CD and can be manually resolved. The quick precipitation of benzil can also produce racemic mixture **Section 2.2**.

6.3.8 Benzil Viedma ripening (attrition-enhanced deracemization)

At room temperature, racemic benzil powder (2.5 g) in saturated benzil solution (1 mL in acetone) was stirred with a magnetic stir bar (PTFE magnetic stirring rod, ring shape, diameter: 3 mm, length 13 mm) with 0.5 mm ceramic beads (3 g). The stirring speed was 800 rpm. Every 15 minutes, 100 μL of slurry mixture was transferred to a filter paper on a watch glass with a micropipette. The sample was dried at 80 ℃ for 5 minutes and mixed with nujol (15% wt/wt). A total weight of 0.09 – 0.10 g nujol mixture was transferred in the center of a quartz plate (diameter: 2 cm, thickness: 2 mm) and pressed carefully with another quartz plate of the same size. The two quartz plates were gently pressed together to remove bubbles from the sample before placing the sample in the cell holder.

6.3.9 Decacyclene viedma ripening

A 20 mL scintillation vial containing 0.10 g racemic decacyclene solid (GTI Laboratories Supplies, 98% decacyclene), 3.00 g ceramic beads (0.3 mm) and 4 mL nitrobenzene solution with a stir bar (PTFE magnetic stirring rod, ring shape, diameter: 3 mm, length 13 mm) was sealed and placed in a sand bath on a hot plate. The hot plate was set to 80℃ and the mixture was stirred at 1000 rpm/min. The stir bar used in this experiment was 10 mm long with a ring in the middle.

About 120 μL of the slurry was removed with a pipette at specified times and the light brown slurry was centrifuged (INTERNATIONAL EQUIPMENT Co., International Clinical Centrifuge Model CL) at 700 rpm in an Ependorf tube until the solid decacyclene settled at the bottom of the dark clear liquid. After removing the top layer of liquid, the precipitate was transferred to a glass slide. The collected sample was air dried overnight in the fume hood. The chiral amplification process can take 15 days or longer.

Dried decacyclene scraped from glass slide was mixed with the dried potassium bromide (3 days, 120℃) to make a 70 mg KBr pellet. The 10-mm diameter pellet containing (0.8 g; 0.5% (wt/wt) decacyclene and KBr mixed thoroughly using a mortar and pestle.

6.3.10 Slow evaporation of epsomite

The magnesium sulfate is 100 wt/wt% of Epsom salt in deionized water. The solution was heated to boiling and stirred in a beaker (500 mL; *ca*. 10 diameter) with a magnetic stir bar. In the set of no chiral additive experiment, additive is borax 0.06 M. In the set of chiral additive experiments with asparagine (0.18 M), the borax

is 0.06 M. Solution cooled to room temperature (*ca*. 22-24℃) after distributed in 100 mL TLG ® beakers evenly, and beaker sealed by plastic wrap with 6-8 holes. The 40 mL beakers on stable surface took 14 days or more for crystallization. Crystallization typically took between 14-30 days, although in some cases, it could take longer. One or more crystals with the desired morphology formed at the bottom of beaker.

The statistics of each enantiomorph for each individual experiment were analyzed with “t-test: paired two samples for means” in excel. The influence of additives compared between the left-handed crystal count yield from experiments with no chiral additives and the corresponding chiral additives with "t-test: two-sample assuming equal variances". More details in **section 8.1**.

6.3.11 Slow evaporation of decacyclene

A 20 mL vial with 0.05 g of decacyclene solid (GTI Laboratories Supplies, 98% decacyclene) was added 0.5 mL of solvent or solvent mixture (1:1 ratio to benzene). The vial was capped and heated up to boil on the hotplate while constantly swirling the vial. If the solution starts to boil but there is still solid at the bottom, an extra 0.5 mL solvent was added until all solid dissolved. The solution slowly cools down to room temperature on the hot plate before removing the cap. The solution slow evaporated in the fumehood. The crystallization may take 3-5 days. The crystals were carefully filtered from the solution with filter paper, or all the crystals were put on filter paper in a petri dish.

6.3.12 Visualization of crystal morphology

The prepared crystals of epsomite were collected. Those crystals have distinctive morphology and were resolved manually. Other crystals can be resolved based on the positive or negative-CD signal, or the color changed under the polarized filter along the clockwise rotation. The information would be compared with relative literature as needed. The crystal model was built with information posted on Cambridge Crystallographic Data Centre (CCDC) or Crystallography Open Database (COD), and sometimes with the information provided by the x-ray diffractometer with the help of Dr. Scott Bohle.

6.3.13 X-ray crystallography

The prepared crystal in millimeter scale were chosen for obtaining absolute configuration and the Flack parameter. The morphology of crystals would be observed under microscope before processing the measurement. The chosen crystal was fixed on the tip of a glass fiber and the information of x-ray diffraction was collected by Dr. Scott Bohle (McGill University).

7 Reference

(1) Fecher, G. H.; Kübler, J.; Felser, C. Chirality in the solid state: chiral crystal structures in chiral and achiral space groups. *Materials* **2022**, *15* (17), 5812.

(2) Szurgot, J.; Szurgot, M. Enantiomorphism in sodium chlorate crystals. *Cryst. Res. Technol.* **1995**, *30* (1), 71-79 (acccessed 2022/06/18).

(3) Szurgot, M. Chiral symmetry breaking in unstirred crystallization. *Cryst. Res. Technol.* **2012**, *47* (1), 109-114 (acccessed 2022/11/15).

(4) Kipping, F. S.; Pope, W. J. Enantiomorphism. *J. Chem. Soc., Trans.* **1898**, *73*, 606-617.

(5) Blackmond, D. G. The origin of biological homochirality. *Cold Spring Harb. perspect. biol.* **2010**, *2* (5), a002147.

(6) Nguyen, L. A.; He, H.; Pham-Huy, C. Chiral drugs: an overview. *Int. J, Biomed. Sci.* **2006**, *2* (2), 85-100.

(7) Gal, J. The discovery of biological enantioselectivity: Louis Pasteur and the fermentation of tartaric acid, 1857 - A review and analysis 150 yr later. *Chirality* **2008**, *20*, 5-19.

(8) Karnik, A. V.; Hasan, M. Stereochemistry: A Three-Dimensional Insight. In *Stereochemistry*, Karnik, A. V., Hasan, M. Eds.; Elsevier, 2021.

(9) Gernez, M. D. *Sur la cristallisation des substances hémiédriques*; Académie des sciences, Centre national de la recherche, scientifique, 1868.

(10) Clevers, S.; Coquerel, G. Kryptoracemic compound hunting and frequency in the cambridge structural database. *CrystEngComm* **2020**, *22* (43), 7407-7419.

(11) Bak, S. Y.; Coquerel, G.; Kim, W.-S.; Park, B. J. Solution volume effects on spontaneous chiral symmetry breaking of sodium chlorate crystals. *J. Phys. Chem. Lett.* **2023**, *14* (3), 785-790.

(12) Ye, X.; Li, B.; Wang, Z.; Li, J.; Zhang, J.; Wan, X. Tuning organic crystal chirality by the molar masses of tailored polymeric additives. *Nat. Commun.* **2021**, *12* (1), 6841.

(13) Mislow, K.; Siegel, J. Stereoisomerism and local chirality. *J. Am. Chem. Soc.* **1984**, *106* (11), 3319-3328.

(14) Brock, C. P.; Dunitz, J. D. Towards a grammar of crystal packing. *Chem. Mater* **1994**, *6* (8), 1118-1127.

(15) Moss, G. P. Basic terminology of stereochemistry (IUPAC Recommendations 1996). *Pure. Appl. Chem.* **1996**, *68* (12), 2193-2222 (acccessed 2023-06-19).

(16) Lee, C.; Weber, J. M.; Rodriguez, L. E.; Sheppard, R. Y.; Barge, L. M.; Berger, E. L.; Burton, A. S. Chirality in organic and mineral systems: A review of reactivity and alteration processes relevant to prebiotic chemistry and life detection missions. In *Symmetry*, 2022; Vol. 14.

(17) Reusch, W. *Virtual Textbook of Organic Chemistry*; Michigan State University, 1999.

(18) Ouellette, R. J.; Rawn, J. D. Carbohydrates. In *Principles of organic chemistry*, Ouellette, R. J., Rawn, J. D. Eds.; Elsevier, 2015; 343-370.

(19) Bentley, R. Are fischer projection formulas really necessary? *Biochem. Educ.* **1997**, *25* (4), 216-220.

(20) Ramsay, O. B. Stereochemistry. In *Nobel prize topics in chemistry*, Vol. 2; Heyden & Son, Incorporated, 1981; 69-80.

(21) Pidcock, E. Achiral molecules in non-centrosymmetric space groups. *Chem. Commun.* **2005**, (27), 3457-3459.

(22) Nakagawa, K.; Martin, A. T.; Nichols, S. M.; Murphy, V. L.; Kahr, B.; Asahi, T. Optical Activity Anisotropy of Benzil. *J. Phys. Chem. C* **2017**, *121* (45), 25494-25502.

(23) Gabe, E. J.; Le Page, Y.; Lee, F. L.; Barclay, L. R. C. The structure of 2,2',4,4',6,6'-hexa-tert-butylbenzil. *Acta Crystallogr. B* **1981**, *37* (1), 197-200 (acccessed 2023/07/13).

(24) Bonner, W. A. Enantioselective autocatalysis. V. The spontaneous resolution of tri-o-thymotide. *Orig. Life Evol. Biosph.* **1999**, *29* (3), 317-328.

(25) Buhse, T.; Cruz, J. M.; Noble-Teran, M. E.; Hochberg, D.; Ribo, J. M.; Crusats, J.; Micheau, J. C. Spontaneous Deracemizations. *Chem Rev* **2021**, *121* (4), 2147-2229.
(26) Walsh, M. P.; Barclay, J. A.; Begg, C. S.; Xuan, J.; Johnson, N. T.; Cole, J. C.; Kitching, M. O. Identifying a hidden conglomerate chiral pool in the CSD. *J. Am. Chem. Soc.* **2022**, *2* (10), 2235-2250.
(27) Vantomme, G.; Crassous, J. Pasteur and chirality: a story of how serendipity favors the prepared minds. *Chirality* **2021**, *33* (10), 597-601 (acccessed 2023/05/28).
(28) Coquerel, G. Preferential crystallization. *Top. Curr. Chem.* **2007**, *269*, 1-51.
(29) Szurgot, J.; Szurgot, M. On the nature of growth hillocks on sodium chlorate crystals. *Cryst. Res. Technol.* **1994**, *29* (6), 829-836 (acccessed 2023/03/02).
(30) Sögütoglu, L. C.; Steendam, R. R. E.; Meekes, H.; Vlieg, E.; Rutjes, F. P. J. T. Viedma ripening: a reliable crystallisation method to reach single chirality. *Chem. Soc. Rev.* **2015**, *44* (19), 6723-6732.
(31) Viedma, C.; Cintas, P. Homochirality beyond grinding: deracemizing chiral crystals by temperature gradient under boiling. *Chem. Commun.* **2011**, *47* (48), 12786-12788.
(32) Van Dongen, S. W.; Baglai, I.; Leeman, M.; Kellogg, R. M.; Kaptein, B.; Noorduin, W. L. Rapid deracemization through solvent cycling: proof-of-concept using a racemizable conglomerate clopidogrel precursor. *Chem. Commun.* **2023**, *59* (26), 3838-3841.
(33) Pasteur, L. Sur les relations qui peuvent exister entre la forme crystalline, la composition chimique et le sens de la polarization rotatoire. *Ann. Chim. Phys.* **1848**, *24*, 442-459.
(34) Sato, I.; Kadowaki, K.; Ohgo, Y.; Soai, K. Highly enantioselective asymmetric autocatalysis induced by chiral ionic crystals of sodium chlorate and sodium bromate. *J. Mol. Catal.* **2004**, *216* (2), 209-214.
(35) Uemura, N.; Toyoda, S.; Shimizu, W.; Yoshida, Y.; Mino, T.; Sakamoto, M. Absolute asymmetric synthesis involving chiral symmetry breaking in diels–alder reaction. In *Symmetry*, 2020; Vol. 12, p 910.
(36) Rybak, W. K.; Skarżyńska, A. Tuning enantioselectivity for crystallization-induced asymmetric synthesis of a conglomerating oxo-rhenium(v) complex. *New J. Chem.* **2012**, *36* (10), 1966-1968.
(37) Soai, K.; Niwa, S.; Hori, H. Asymmetric self-catalytic reaction. self-production of chiral 1-(3-pyridyl)alkanols as chiral self-catalysts in the enantioselective addition of dialkylzinc reagents to pyridine-3-carbaldehyde. *J. Chem. Soc. Chem. Commun.* **1990**, (14), 982-983.
(38) Rekis, T. Crystallization of chiral molecular compounds: what can be learned from the cambridge structural database? *Acta Crystallogr., Sec. B* **2020**, *76* (3), 307-315 (acccessed 2023/07/23).
(39) Jacques, J.; Collet, A.; Wilen, S. H. *Enantiomers Racemates and Resolutions*; Wiley, 1981.
(40) Koshima, H.; Fukano, M.; Ojima, N.; Johmoto, K.; Uekusa, H.; Shiro, M. Absolute asymmetric photocyclization of triisopropylbenzophenone derivatives in crystals and their morphological changes. *J. Org. Chem.* **2014**, *79* (7), 3088-3093.
(41) Matsuura, T.; Koshima, H. Introduction to chiral crystallization of achiral organic compounds: Spontaneous generation of chirality. . *Photochem. Photobiol. C: Photochem.* **2005**, *6* (1), 7-24.
(42) Buhse, T.; Cruz, J.-M.; Noble-Terán, M. E.; Hochberg, D.; Ribó, J. M.; Crusats, J.; Micheau, J.-C. Spontaneous deracemizations. *Chem. Rev.* **2021**, *121* (4), 2147-2229.
(43) Walsh, M. P.; Barclay, J. A.; Begg, C. S.; Xuan, J.; Kitching, M. O. Conglomerate crystallization in the cambridge structural database (2020–2021). *Cryst. Growth Des.* **2023**, *23* (4), 2837−2844.
(44) Groom, C. R.; Bruno, I. J.; Lightfoot, M. P.; Ward, S. C. The cambridge structural database. *Acta Crystallogr. B* **2016**, *72* (2), 171-179.
(45) Sivakumar, R. The role of conglomerate crystallization in spontaneous resolution and chiral amplification. Concordia University, Concordia University, 2016. https://spectrum.library.concordia.ca/id/eprint/981773/1/Sivakumar_MSc_F2016.pdf.
(46) Addadi, L.; Berkovitch-Yellin, Z.; Weissbuch, I.; van Mil, J.; Shimon, L. J. W.; Lahav, M.; Leiserowitz, L. Growth and dissolution of organic crystals with "Tailor-Made" inhibitors—implications in

stereochemistry and materials science. *Angew. Chem. Int. Ed. Engl.* **1985**, *24* (6), 466-485 (acccessed 2023/07/13).
(47) Winn, D.; Doherty, M. F. Modeling crystal shapes of organic materials grown from solution. *AICHE J.* **2000**, *46*, 1348-1367.
(48) Rousseau, R. W. Crystallization Processes☆. In *Reference module in chemistry, molecular sciences and chemical engineering*, Elsevier, 2014; 91-119.
(49) Dufet, H. Recherches expérimentales sur l'existence de la polarisation rotatoire dans les cristaux biaxes. *Bull. Soc. minéral. Fr.* **1904**, *6*, 168 -174.
(50) Tutton, A. E. H. Some recent progress in chemical and structural crystallography. *Sci. prog. twent. century* **1906**, *1* (1), 91-116 (acccessed 2023/07/27/).
(51) Choudhary, R. N. P.; Nelmes, R. J.; Rouse, K. D. A room-temperature neutron-diffraction study of NaH2PO4. *Chem. Phys. Lett.* **1981**, *78* (1), 102-105.
(52) Gaubert, M. P. Contribution à l'étude des faces cristallines. *Bull. Mineral.* **1904**, *1*, 6-63.
(53) Glusker, J. P.; Lewis, M.; Rossi, M. *Crystal structure analysis for chemists and biologists*; John Wiley & Sons, 1996.
(54) Gladstone, J. H. On circular polarization. A discourse delivered to the member of the chemcial society of London. *Q. J. Chem. Soc.* **1861**, *13* (3), 254-270.
(55) Beevers, C. A.; McDonald, T. R. R.; Robertson, J. H.; Stern, F. The crystal structure of sucrose. *Acta Crystallogr.* **1952**, *5* (5), 689-690.
(56) Schmieder, P.; Denysenko, D.; Grzywa, M.; Baumgärtner, B.; Senkovska, I.; Kaskel, S.; Sastre, G.; van Wüllen, L.; Volkmer, D. CFA-1: the first chiral metal–organic framework containing kuratowski-type secondary building units. *Dalton Trans.* **2013**, *42* (30), 10786-10797.
(57) Nagasato, S.; Katsuki, I.; Motoda, Y.; Sunatsuki, Y.; Matsumoto, N.; Kojima, M. Correlation among crystal shape, absolute configuration, and circular dichroism spectrum of enantiomorphs of Tris[2-(((2-phenylimidazol-4-yl)methylidene)amino)ethyl]- aminemetal(II) Nitrate−Methanol (1/1). *Inorg. Chem.* **2001**, *40* (11), 2534-2540.
(58) G. Kostyanovsky, R.; R. Kostyanovsky, V.; K. Kadorkina, G.; A. Lyssenko, K. Wedekind–fock–havinga salt Me(Et)N+(All)PhI– · CHCl3 as historically the first object for absolute asymmetric synthesis: spontaneous resolution, structure and absolute configuration. *Mendeleev Commun.* **2001**, *11* (1), 1-5.
(59) Sangwal, K.; Szurgot, M.; Szczepaniak, M. On the enantiomorphism in potassium bichromate crystals. *J. Cryst. Growth* **1986**, *79* (1), 185-191.
(60) Swanson, H.; Tatge, E.; Fuyat, R.; Patterns, S. X.-r. D. P. US Dept. of Commerce. *National Bureau of Standards, Washington, DC* **1953**.
(61) Priya, R.; Krishnan, S.; Raj, C. J.; Das, S. J. Growth and characterization of NLO active lithium sulphate monohydrate single crystals. *Cryst. Res. Technol.* **2009**, *44* (12), 1272-1276 (acccessed 2023/07/31).
(62) Azumaya, I.; Okamoto, I.; Nakayama, S.; Tanatani, A.; Yamaguchi, K.; Shudo, K.; Kagechika, H. A chiral N-methylbenzamide: spontaneous generation of optical activity. *Tetrahedron* **1999**, *55* (37), 11237-11246.
(63) Sivakumar, R.; Askari, M. S.; Woo, S.; Madwar, C.; Ottenwaelder, X.; Bohle, D. S.; Cuccia, L. A. Homochiral crystal generation via sequential dehydration and Viedma ripening. *Cryst. Eng. Comm.* **2016**, *18* (23), 4277-4280.
(64) Chandrasekhar, S.; Gorla, S. K. Novel cis–trans enantiomeric conglomerates: triage and absolute configurations via anomalous X-ray scattering. A photochemical second order asymmetric transformation. *Tetrahedron Asymm.* **2006**, *17* (15), 2247-2251.
(65) Li, W.-K.; Zhou, G.-D.; Wai Mak, T. C. Symmetry in crystals. In *Advanced Structural Inorganic Chemistry*; Li, W.-K., Zhou, G.-D., Mak, T., Eds.; Oxford University Press, 2008.

(66) Tanaka, R. *Cinnabar (HgS)*. Hudson Institute of Mineralogy, 2010. https://www.mindat.org/photo-334001.html (accessed July 31, 2023).
(67) An, G.; Yan, P.; Sun, J.; Li, Y.; Yao, X.; Li, G. The racemate-to-homochiral approach to crystal engineering via chiral symmetry breaking. *CrystEngComm* **2015**, *17* (24), 4421-4433.
(68) Wong, S. Y.; Hartel, R. W. Crystallization in lactose refining-A review. *J. Food Sci.* **2014**, *79* (3), R257-R272 (acccessed 2023/07/31).
(69) Collet, A.; Brienne, M. J.; Jacques, J. Optical resolution by direct crystallization of enantiomer mixtures. *Chem. Rev.* **1980**, *80* (3), 215-230.
(70) Read, J.; Cook, A. M. R.; Shannon, M. I. CCXCIV.—Researches in the menthone series. Part III. Optically inactive menthylamines. *J. Chem. Soc.* **1926**, *129*, 2223-2234.
(71) Tanaka, K.; Takenaka, H.; Caira, M. R. Resolution of 4-oxoazetidin-2-yl benzoate by inclusion crystallization with an optically active host compound. *Tetrahedron: Asymmetry* **2006**, *17* (15), 2216-2219.
(72) Cai, L.; Li, Y.; Yu, C.; Ji, H.; Liu, Y.; Liu, S. Spontaneous resolution of a chiral polyoxometalate: Synthesis, crystal structures and properties. *Inorganica Chimica Acta* **2009**, *362* (8), 2895-2899.
(73) Hager, O.; Llamas‐Saiz, A. L.; Foces‐Foces, C.; Claramunt, R. M.; López, C.; Elguero, J. Complexes between 1, 1′‐binaphthyl‐2, 2′‐dicarboxylic acid and pyrazoles: a case of manual sorting of conglomerate crystals (triage). *Helv. Chim. Acta.* **1999**, *82* (12), 2213-2230.
(74) Katzir, S. The emergence of the principle of symmetry in physics. *Historical Studies in the Physical and Biological Sciences* **2004**, *35* (1), 35-65 (acccessed 2023/08/08/).
(75) Kubbinga, H. Crystallography from Haüy to Laue: controversies on the molecular and atomistic nature of solids. *Acta Crystallogr., Sect. A: Found Chrstallogr.* **2012**, *68* (1), 3-29.
(76) Tobe, Y. The reexamination of Pasteur's experiment in Japan. *Mendeleev Commun.* **2003**, *13* (3), 93-94.
(77) Kauffman, G. B.; Myers, R. D. The resolution of racemic acid: A classic stereochemical experiment for the undergraduate laboratory. *Journal of Chemical Education* **1975**, *52* (12), 777.
(78) Evgenii, K.; Wolfram, T. The role of quartz in the origin of optical activity on earth. *Orig. Life Evol. Biosph.* **2000**, *30* (5), 431-434.
(79) Pasteur, L. *M. Pasteur's Reply to M. Wyrouboff*; Griffin, Bohn and Company, 1884.
(80) Im, S. W.; Ahn, H.-Y.; Kim, R. M.; Cho, N. H.; Kim, H.; Lim, Y.-C.; Lee, H.-E.; Nam, K. T. Chiral surface and geometry of metal nanocrystals. *Adv. Mater* **2020**, *32* (41), 1905758 (acccessed 2023/07/14).
(81) Jacques, J.; Collet, A.; Wilen, S. H. *Enantiomers, racemates, and resolutions*; R.E. Krieger, 1994.
(82) Hashimoto, A.; Nishikawa, T.; Oka, T.; Takahashi, K. Endogenous d-serine in rat brain: N-methyl-d-aspartate receptor-related distribution and aging. *J. Neurochem.* **1993**, *60* (2), 783-786 (acccessed 2023/06/13).
(83) Busch, K. W.; Busch, M. A. Chapter 3 - Light polarization and signal processing in chiroptical instrumentation. In *Chiral Analysis (Second Edition)*, Polavarapu, P. L. Ed.; Elsevier, 2018; 73-151.
(84) Barron, L. D. *Molecular light scattering and optical activity*; Cambridge University Press, 2004.
(85) Klein, C.; Hurlbut, C. S. *The manual of mineral science*; J. Wiley, 2002.
(86) Buckingham, A. D.; Stiles, P. J. Theory of natural optical activity. *Acc. Chem. Res.* **1974**, *7* (8), 258-264.
(87) Tanaka, Y.; Takeuchi, T.; Lovesey, S. W.; Knight, K. S.; Chainani, A.; Takata, Y.; Oura, M.; Senba, Y.; Ohashi, H.; Shin, S. Right handed or left handed? Forbidden X-ray diffraction reveals chirality. *Phys. Rev. Lett.* **2008**, *100* (14), 145502.
(88) Flack, H. D. Chiral and achiral crystal structures. *Helv. Chim. Acta* **2003**, *86* (4), 905-921 (acccessed 2023/06/05).
(89) Valentín-Pérez, Á.; Rosa, P.; Hillard, E. A.; Giorgi, M. Chirality determination in crystals. *Chirality* **2022**, *34* (2), 163-181 (acccessed 2023/07/16).

(90) Harris, D. C. *Quantitative chemical analysis*; Macmillan Learning, 2015.
(91) Flack, H. Louis Pasteur's discovery of molecular chirality and spontaneous resolution in 1848, together with a complete review of his crystallographic and chemical work. *Acta Crystallographica Section A* **2009**, *65* (5), 371-389.
(92) El-Hachemi, Z.; Escudero, C.; Arteaga, O.; Canillas, A.; Crusats, J.; Mancini, G.; Purrello, R.; Sorrenti, A.; D'Urso, A.; Ribo, J. M. Chiral sign selection on the J-aggregates of diprotonated tetrakis-(4-sulfonatophenyl)porphyrin by traces of unidentified chiral contaminants present in the ultra-pure water used as solvent. *Chirality* **2009**, *21* (4), 408-412 (acccessed 2023/08/08).
(93) Quesada-Moreno, M. M.; Avilés-Moreno, J. R.; López-González, J. J.; Jacob, K.; Vendier, L.; Etienne, M.; Alkorta, I.; Elguero, J.; Claramunt, R. M. Supramolecular organization of perfluorinated 1H-indazoles in the solid state using X-ray crystallography, SSNMR and sensitive (VCD) and non sensitive (MIR, FIR and Raman) to chirality vibrational spectroscopies. *Phys. Chem. Chem. Phys.* **2017**, *19* (2), 1632-1643.
(94) Alkorta, I.; Elguero, J. The strange case of achiral compounds which were reported to always crystallize in the same chiral group. *Struct. Chem.* **2019**, *30* (3), 633-636.
(95) Lennartson, A.; Håkansson, M. Total spontaneous resolution of five-coordinate complexes. *Angew. Chem. Int. Ed.* **2009**, *48* (32), 5869-5871 (acccessed 2023/08/08).
(96) Gao, C. Y.; Wang, F.; Tian, H. R.; Li, L. J.; Zhang, J.; Sun, Z. M. Particular handedness excess through symmetry-breaking crystallization of a 3D cobalt phosphonate. *Inorg. Chem.* **2016**, *55* (2), 537-539.
(97) Lennartson, A.; Håkansson, M. Absolute asymmetric synthesis of five-coordinate complexes. *New J. Chem.* **2015**, *39* (8), 5936-5943.
(98) Pocklington, H. C. Cheirality of form of crystals of epsom salt. *Nature* **1906**, *73* (1890), 270.
(99) Kondepudi, D. K.; Kaufman, R. J.; Singh, N. Chiral symmetry breaking in sodium chlorate crystallizaton. *Science* **1990**, *250* (4983), 975-976.
(100) Diniz, P. C.; Wattis, J. A. D.; da Costa, F. P. Mathematical Models of Chiral Symmetry-breaking – A Review of General Theories, and Adiabatic Approximations of the APED System. *Origins of Life and Evolution of Biospheres* **2022**, *52* (4), 183-204.
(101) Doran, P. M. Chapter 11 - Unit operations. In *Bioprocess Engineering Principles (Second Edition)*, Doran, P. M. Ed.; Academic Press, 2013; 445-595.
(102) Erdemir, D.; Lee, A. Y.; Myerson, A. S. *Handbook of industrial crystallization*; Cambridge University Press, 2019.
(103) Prasad, M. R.; Deb, P. K.; Chandrasekaran, B.; Maheshwari, R.; Tekade, R. K. Chapter 3 - Basics of crystallization process applied in drug exploration. In *Dosage Form Design Parameters*, Tekade, R. K. Ed.; Vol. 2; Academic Press, 2018; 67-103.
(104) Niedermaier, T.; Schlenk, J. W. Zur optischen aktivität der natriumchlorat- und natriumbromat-kristalle. *Chem. Ber.* **1972**, *105* (10), 3470-3478 (acccessed 2022/06/18).
(105) Pagni, R. M.; Compton, R. N. Asymmetric synthesis of optically active sodium chlorate and bromate crystals. *Cryst. Growth Des.* **2002**, *2* (4), 249-253.
(106) Chalk, S. J. *Asymmetric transformation*, Compiled by Online version (2019-) ed.; A. D. McNaught and A. Wilkinson. Blackwell Scientific Publications, 1997.
(107) McBride, J. M.; Carter, R. L. Spontaneous resolution by stirred crystallization. *Angew. Chem. Int. Ed. Engl.* **1991**, *30* (3), 293-295.
(108) Cartwright, J. H. E.; Piro, O.; Tuval, I. Ostwald ripening, chiral crystallization, and the common-ancestor effect. *Phys. Rev. Lett.* **2007**, *98* (16), 165501.
(109) Blackmond, D. G. "Chiral amnesia" as a driving force for solid-phase homochirality. *Chemistry* **2007**, *13* (12), 3290-3295.

(110) Viedma, C.; McBride, J. M.; Kahr, B.; Cintas, P. Enantiomer‐specific oriented attachment: formation of macroscopic homochiral crystal aggregates from a racemic system. *Angew. Chem.* **2013**, *125* (40), 10739-10742.
(111) Sivakumar, R.; Kwiatoszynski, J.; Fouret, A.; Nguyen, T. P. T.; Ramrup, P.; Cheung, P. S. M.; Cintas, P.; Viedma, C.; Cuccia, L. A. Enantiomer-specific oriented attachment of guanidine carbonate crystals. *Cryst. Growth Des.* **2016**, *16* (7), 3573-3576.
(112) Viedma, C. Chiral symmetry breaking during crystallization: complete chiral purity induced by nonlinear autocatalysis and recycling. *Phys. Rev. Lett.* **2005**, *94* (6), 065504.
(113) Mills, R. D.; Ratner, J. J.; Glazner, A. F. Experimental evidence for crystal coarsening and fabric development during temperature cycling. *Geology* **2011**, *39* (12), 1139-1142 (acccessed 4/3/2023).
(114) Belletti, G.; Schuurman, J.; Stinesen, H.; Meekes, H.; Rutjes, F. P. J. T.; Vlieg, E. Combining viedma ripening and temperature cycling deracemization. *Cryst. Growth Des.* **2022**, *22* (3), 1874-1881.
(115) Zhang, B.; Sun, X.; Du, P. Designing single chirality via crystallization method: spontaneous chiral symmetry breaking and deracemization. *Mater. Today Chem.* **2023**, *32*, 101636.
(116) Genaev, A. M.; Salnikov, G. E.; Shernyukov, A. V.; Zhu, Z.; Koltunov, K. Y. Enhanced enantiostability of BINOL dimethyl ether under moderate acidic conditions. *Mendeleev Commun.* **2018**, *28* (1), 27-28.
(117) Belletti, G.; Tortora, C.; Mellema, I. D.; Tinnemans, P.; Meekes, H.; Rutjes, F. P. J. T.; Tsogoeva, S. B.; Vlieg, E. Photoracemization-based viedma ripening of a BINOL derivative. *Chem. Eur. J.* **2020**, *26* (4), 839-844 (acccessed 2023/08/10).
(118) Lerdwiriyanupap, T.; Belletti, G.; Tinnemans, P.; Meekes, H.; Rutjes, F. P. J. T.; Vlieg, E.; Flood, A. E. Combining diastereomeric resolution and viedma ripening by using a racemic resolving agent. *EurJOC* **2021**, *2021* (44), 5975-5980 (acccessed 2023/08/10).
(119) Spix, L.; Alfring, A.; Meekes, H.; van Enckevort, W. J. P.; Vlieg, E. Formation of a salt enables complete deracemization of a racemic compound through viedma ripening. *Cryst. Growth Des.* **2014**, *14* (4), 1744-1748.
(120) Spix, L.; Meekes, H.; Blaauw, R. H.; van Enckevort, W. J. P.; Vlieg, E. Complete deracemization of proteinogenic glutamic acid using viedma ripening on a metastable conglomerate. *Cryst. Growth Des.* **2012**, *12* (11), 5796-5799.
(121) Viedma, C. Experimental evidence of chiral symmetry breaking in crystallization from primary nucleation. *J. Cryst. Growth* **2004**, *261* (1), 118-121.
(122) Maggioni, G. M.; Mazzotti, M. Modelling the stochastic behaviour of primary nucleation. *Faraday Discussions* **2015**, *179* (0), 359-382.
(123) McLaughlin, D. T.; Nguyen, T. P. T.; Mengnjo, L.; Bian, C.; Leung, Y. H.; Goodfellow, E.; Ramrup, P.; Woo, S.; Cuccia, L. A. Viedma ripening of conglomerate crystals of achiral molecules monitored using solid-state circular dichroism. *Cryst. Growth Des.* **2014**, *14* (3), 1067-1076.
(124) Kodera, T.; Kobari, M.; Hirasawa, I. Experimental estimation of primary and secondary nucleation kinetics of antisolvent crystallization as measured by induction time. *Org. Process Res. Dev.* **2019**, *23* (12), 2724-2732.
(125) Copithorne-Crainey, C. W.; Armstrong, F. J.; Bussemaker, M.; Lee, J. Use of enantiomeric properties of sodium chlorate to assess primary and secondary nucleation under sonication. *Ultrason Sonochem* **2021**, *79*, 105763.
(126) Nalesso, S.; Bussemaker, M. J.; Sear, R. P.; Hodnett, M.; Lee, J. A review on possible mechanisms of sonocrystallisation in solution. *Ultrason. Sonochem.* **2019**, *57*, 125-138.
(127) Chow, R.; Blindt, R.; Chivers, R.; Povey, M. A study on the primary and secondary nucleation of ice by power ultrasound. *Ultrasonics* **2005**, *43* (4), 227-230.

(128) Noorduin, W. L.; Izumi, T.; Millemaggi, A.; Leeman, M.; Meekes, H.; Van Enckevort, W. J. P.; Kellogg, R. M.; Kaptein, B.; Vlieg, E.; Blackmond, D. G. Emergence of a single solid chiral state from a nearly racemic amino acid derivative. *J. Am. Chem. Soc.* **2008**, *130* (4), 1158-1159.
(129) Ho, D. M.; Pascal, R. A. Decacyclene: a molecular propeller with helical crystals. *Chem. Mater* **1993**, *5* (9), 1358-1361.
(130) Kondepudi, D. K.; Bullock, K. L.; Digits, J. A.; Hall, J. K.; Miller, J. M. Kinetics of chiral symmetry breaking in crystallization. *J. Am. Chem. Soc.* **1993**, *115* (22), 10211-10216.
(131) Killalea, C. E.; Amabilino, D. B. Stereochemistry and twisted crystals. *Isr. J. Chem.* **2021**, *61* (9-10), 629-644 (acccessed 2023/08/10).
(132) Li, C.; Shtukenberg, A. G.; Vogt-Maranto, L.; Efrati, E.; Raiteri, P.; Gale, J. D.; Rohl, A. L.; Kahr, B. Why Are Some Crystals Straight? *The Journal of Physical Chemistry C* **2020**, *124* (28), 15616-15624.
(133) Fortes, A. D. From surrey to the moons of jupiter (via mars): the story of epsomite. 2005.
(134) M., K. Zur morphologie des bittersalzes. *Neues Jahrb. Geol. Paläontol.* **1929**, *59*, 273-296.
(135) Rubbo, M.; Aquilano, D.; Franchini-Angela, M.; Sgualdino, G. Growth morphology of epsomite (MgSO4·7H2O). *J. Cryst. Growth* **1985**, *71* (3), 470-482.
(136) Ruiz-Agudo, E.; Rodriguez-Navarro, C. Suppression of salt weathering of porous limestone by borax-induced promotion of sodium and magnesium sulphate crystallization. *Geol. Soc. Spec. Publ.* **2010**, *331* (1), 93-102 (acccessed 2023/07/28).
(137) Calleri, M.; Gavetti, A.; Ivaldi, G.; Rubbo, M. Synthetic epsomite, MgSO4.7H2O: absolute configuration and surface features of the complementary {111} forms. *Acta Crystallogr. B* **1984**, *40* (3), 218-222.
(138) Me, J.-J.; Xu, D.-J.; Wu, J.-Y.; Chiang, M. Y. Separation and structure of chiral s-malic acid hydrate. *Chin. J. Chem.* **2002**, *20* (4), 395-398 (acccessed 2023/07/31).
(139) Noorduin, W. L.; Vlieg, E.; Kellogg, R. M.; Kaptein, B. From ostwald ripening to single chirality. *Angew. Chem. Int. Ed. Engl.* **2009**, *48* (51), 9600-9606.
(140) Belyustin, A. V. R., É. D. Production of crystllization nuclei in the presence of a seed crystal. *Growth of Crystals* **1966**, *4*, 3-5.
(141) Steed, K. M.; Steed, J. W. Packing problems: high Z' crystal structures and their relationship to cocrystals, inclusion compounds, and polymorphism. *Chem. Rev.* **2015**, *115* (8), 2895-2933.
(142) Crystallography, O. D. o. *Polymorphism*. Online Dictionary of Crystallography, https://dictionary.iucr.org/Polymorphism (accessed 2023 August 03).
(143) El Hachemi, Z.; Crusats, J.; Ribo, J. M.; McBride, J.; Veintemillas-Verdaguer, S. Metastability in supersaturated solution and transition towards chirality in the crystallization of NaClO3. *Angew. Chem., Int. Ed.* **2011**, *50*, 2359-2363.
(144) Heldebrant, D. J.; Karkamkar, A.; Linehan, J. C.; Autrey, T. Synthesis of ammonia borane for hydrogen storage applications. *Energy Environ. Sci.* **2008**, *1* (1), 156-160.
(145) Stark, K.-A. S.; Gascooke, J. R.; Gibson, C. T.; Lenehan, C. E.; Bonnar, C.; Fitzgerald, M.; Kirkbride, K. P. Xylitol pentanitrate – its characterization and analysis. *Forensic Sci. Int.* **2020**, 110472.
(146) Kim, H. S.; Jeffrey, G. A. The crystal structure of xylitol. *Acta Crystallogr. B* **1969**, 2607–2613.
(147) Wolfrom, M. L.; Kohn, E. J. Crystalline xylitol. *J. Am. Chem. Soc.* **1942**, 1739–1739.
(148) Wouters, J.; Van Meervelt, L. Classroom experiments with artificial sweeteners: growing single crystals and simple calorimetry. *Acta Crystallographica Section E* **2022**, *78* (9), 874-879.
(149) Safari, F.; Katrusiak, A. Structure–property relationships of molecular shape and orientation with compression and expansion of xylitol. *Acta Crystallogr. B* **2021**, 205-210.

8 Appendix

8.1 The statistics of crystal count analysis.

The enantiomorph distribution to be stochastic or non-stochastic was examined in the t-test: paired two samples for means. This test compares the difference between the data of two sample groups, the formation of left-handed and right-handed crystals. The null hypothesis would have lower support when a low p-value is observed.[90] If the p-value of two-tailed is 5%, only 5 out of 100 cases the mean difference between two set of results with the same mean. In other words, the equal distribution between enantiomorphs is only 5%.[90] The t-value of two-tailed depends on the t-value calculated in the **Equation 3**, and p-value ($t_{critical}$) is in the corresponding to the degree of freedom (DOF= n-1) in the t-table.[90]

Equation 3. The t-value of the t-Test: Paired Two Sample for Means.[90]

$$t_{(Paired)} = \frac{|\overline{d}|}{s_d}\sqrt{DOF}$$

The difference between two results for each sample are difference (d_i), the mean difference $\overline{d}$ is the mean of all difference ($\overline{d} = \frac{d_i}{n}$). The sample size is n (*i.e.* the sample 1 has n_1 samples), and the mean of the sample is $\bar{x}$ (*i.e.* the mean of the sample 1 is $\bar{x}_1$). Each individual value in the sample set is x_i or x_j.

The is the sample mean $\bar{x}$: [90]

$$\bar{x} = \frac{\sum_i x_i}{n}$$

The standard deviation s: [90]

$$s_d = \sqrt{\frac{\sum_i (x_i - \bar{x})^2}{n-1}}$$

Besides, the statistical significance between different additives was analyzed with the t-test: two-sample assuming equal variances. It is a test assuming the two variants caused the same impact on both sample groups, about the left-handed crystal count particularly. In this t-test, if the t-value is larger than the t-critical value, the null hypothesis is rejected.[90] The two variances caused significant differences between the two sample groups when the null hypothesis was rejected.[90] The $t_{critical}$ is the value from the t-table with degree of freedom (DOF = $n_1 + n_2 - 2$), assumed the confidential level as 95%, which means this hypothesis is 95%.[90]

Equation 4. The t-value of t-test: two-sample assuming equal variances (t test for comparison of means).[90]

$$\text{t (equal variances)} = \frac{|\bar{x}_1 - \bar{x}_2|}{\text{s\_pooled}} \sqrt{\frac{n_1 n_2}{n_1 + n_2}}$$

The $\bar{x}_1$ and $\bar{x}_2$ are means of sample 1 and sample 2. The standard combined standard deviation (s_pooled) is calculated in the equation bellowed. [90]

$$\text{s\_pooled} = \sqrt{\frac{\sum_{set\ 1}(x_i - \bar{x}_1)^2 + \sum_{set\ 2}(x_j - \bar{x}_2)^2}{n_1 + n_2 - 2}}$$

The t-test: paired two samples for means indicated the epsomite crystallization are non-stochastic crystallization when there are no chiral additives (p-value of two-tailed: 0.0000001%) and when D-asparagine additives and L-asparagine additives (p-value of two-tailed: 1% and 2%) has low concentration 0.06 M. The independent experiments with dominant crystal species as left- and right-handed crystals is 11 to 12 when 0.18 M D-asparagine involved in the experiments. This type of additive makes stochastic crystallization become possible, with 36% p-value of two-tailed in the t-test: paired two samples for means.

(SI) Table 1. The epsomite crystallization with no chiral additive has 0.0000001% possibility (p-value = 0.0000001%) to be stochastic crystallization.

t-Test: Paired Two Sample for Means		
	Variable 1	*Variable 2*
Mean	3	0.11364
Variance	5.612403101	0.10307
Observations	44	44
Pearson Correlation	-0.118912062	
Hypothesized Mean Difference	0	
df	43	
t Stat	7.884712435	
P(T<=t) one-tail	3.45441E-10	
t Critical one-tail	1.681070703	
P(T<=t) two-tail	0.0000001%	
t Critical two-tail	2.016692199	

(SI) Table 2. The epsomite crystallization with 0.18 M L-asparagine additive has 0.00003% possibility (p-value = 0.00003%) to be stochastic crystallization.

t-Test: Paired Two Sample for Means		
	Variable 1	*Variable 2*
Mean	2.25	0.5
Variance	2.238372	0.906977
Observations	44	44
Pearson Correlation	-0.17138	
Hypothesized Mean Difference	0	
df	43	
t Stat	6.089598	
P(T<=t) one-tail	0.00001%	
t Critical one-tail	1.681071	
P(T<=t) two-tail	0.00003%	
t Critical two-tail	2.016692	

(SI) Table 3. The epsomite crystallization with 0.18 M D-asparagine additive has 36% possibility (p-value = 36%) to be stochastic crystallization.

t-Test: Paired Two Sample for Means		
	Variable 1	*Variable 2*
Mean	0.84	1.48
Variance	1.306667	8.176667
Observations	25	25
Pearson Correlation	-0.3452	
Hypothesized Mean Difference	0	
df	24	
t Stat	-0.93393	
P(T<=t) one-tail	18%	
t Critical one-tail	1.710882	
P(T<=t) two-tail	36%	
t Critical two-tail	2.063899	

(SI) Table 4. 0.18 M L-asparagine additive has a significantly different influence in epsomite crystallization compared to no chiral additives. (t-stat > t Critical two-tail)

t-Test: Two-Sample Assuming Equal Variances		
	Variable 1	*Variable 2*
Mean	0.5	0.333333
Variance	0.906977	1.666667
Observations	44	15
Pooled Variance	1.093567	
Hypothesized Mean Difference	0	
df	57	
t Stat	0.533055	
P(T<=t) one-tail	30%	
t Critical one-tail	1.672029	
P(T<=t) two-tail	60%	
t Critical two-tail	2.002465	

(SI) Table 5. 0.18 M D-asparagine additive has a significantly different influence in epsomite crystallization compared to no chiral additives. (t-stat > t Critical two-tail)

t-Test: Two-Sample Assuming Equal Variances		
	Variable 1	*Variable 2*
Mean	1.48	0.333333
Variance	8.176667	1.666667
Observations	25	15
Pooled Variance	5.778246	
Hypothesized Mean Difference	0	
df	38	
t Stat	1.460578	
P(T<=t) one-tail	8%	
t Critical one-tail	1.685954	
P(T<=t) two-tail	15%	
t Critical two-tail	2.024394	

(SI) Table 6. 0.18 M D-asparagine additives and 0.18 M L-asparagine additive need more experiments to estimate if there is a significantly different influence in epsomite crystallization (t-stat ≈ t Critical two-tail)

t-Test: Two-Sample Assuming Equal Variances		
	Variable 1	*Variable 2*
Mean	1.48	0.5
Variance	8.176667	0.906977
Observations	25	44
Pooled Variance	3.511045	
Hypothesized Mean Difference	0	
df	67	
t Stat	2.088237	
P(T<=t) one-tail	2.0%	
t Critical one-tail	1.667916	
P(T<=t) two-tail	4.1%	
t Critical two-tail	1.996008	

8.2 The espsomite count in independent experiments with different additives.

(SI) Table 7. The epsomite crystallization with no chiral additive (achiral additive: borax).

Batch	Concentration (Borax) (M)	The counts of right-handed crystal	The counts of left-handed crystal	ee%
1	0.13	2	0	100%
2	0.13	1	0	100%
3	0.13	1	0	100%
4	0.13	2	0	100%
5	0.13	1	0	100%
6	0.13	1	0	100%
7	0.12	3	0	100%
8	0.13	7	0	100%
9	0.13	7	0	100%

10	0.13	1	0	100%
11-14 (Nicole Paredes-Vegas)	0.13	12	0	100%
	0.13	9	0	100%
	0.13	10	0	100%
	0.13	5	0	100%
15-42 (Evelyn Huaman)	0.13	60	5	85%
43-46 (Dr. Louis A. Cuccia)	0.13	3	0	100%
	0.13	3	0	100%
	0.13	4	0	100%
	0.13	2	0	100%

(SI) Table 8. The epsomite crystallization with L-asparagine as chiral additive.

Batch	Concentration (Borax) (M)	Concentration (L-asparagine) (M)	The counts of right-handed crystal	The counts of left-handed crystal	ee%
1	0.12	0.17	5	0	100%
2	0.12	0.17	2	2	0%
3	0.12	0.17	3	0	100%
4	0.07	0.18	6	0	100%
5	0.07	0.18	2	0	100%
6	0.07	0.18	4	2	33%

7	0.07	0.18	0	1	-100%
8	0.07	0.18	2	1	33%
9	0.07	0.18	1	0	100%
10	0.07	0.18	0	2	-100%
11	0.07	0.18	1	0	100%
12	0.07	0.18	4	1	60%
13	0.07	0.18	1	0	100%
14	0.07	0.18	2	0	100%
15	0.05	0.15	1	5	-67%
16	0.05	0.15	3	0	100%
17	0.06	0.15	2	0	100%
18	0.07	0.18	1	0	100%
19	0.07	0.18	1	0	100%
20	0.07	0.18	4	1	60%
21	0.07	0.18	5	0	100%
22	0.06	0.16	3	0	100%
23	0.06	0.16	3	0	100%
24	0.06	0.16	1	0	100%
25	0.06	0.16	1	0	100%

26-41 (Liu Yafei)	0.06	0.18	2	0	100%
	0.06	0.18	2	0	100%
	0.06	0.18	4	0	100%
	0.06	0.18	1	1	0%
	0.06	0.18	1	0	100%
	0.06	0.18	1	0	100%
	0.06	0.18	5	0	100%
	0.06	0.18	0	2	-100%
	0.06	0.18	3	0	100%
	0.06	0.18	3	0	100%
	0.06	0.18	1	0	100%
	0.06	0.18	1	0	100%
	0.06	0.18	3	0	100%
	0.06	0.18	1	0	100%
	0.06	0.18	3	1	50%
	0.06	0.18	2	0	100%
42-44 (Nicole Paredes-Vegas)	0.06	0.18	1	1	0%
	0.06	0.18	4	1	60%
	0.06	0.18	3	1	50%

(SI) Table 9. The epsomite crystallization with D-asparagine as chiral additive

Batch	Concentration (Borax) (M)	Concentration (D-asparagine) (M)	The counts of right-handed crystal	The counts of left-handed crystal	ee%
1	0.06	0.18	1	0	100%
2	0.06	0.18	0	1	-100%
3	0.06	0.18	0	1	-100%
4	0.07	0.18	1	0	100%
5	0.07	0.18	2	0	100%
6	0.07	0.18	0	1	-100%
7	0.07	0.18	0	1	-100%
8	0.07	0.18	2	1	33%
9	0.07	0.18	1	0	100%
10	0.07	0.18	0	5	-100%
11	0.07	0.18	0	14	-100%
12	0.07	0.18	1	0	100%
13	0.07	0.18	2	0	100%
14	0.07	0.18	0	1	-100%
15	0.07	0.18	0	1	-100%
16	0.07	0.18	2	0	100%
17	0.07	0.18	5	0	100%
18	0.07	0.18	0	3	-100%
19	0.07	0.18	0	2	-100%

20	0.07	0.18	1	1	0%
21	0.07	0.18	1	0	100%
22-25 (Liu Yafei)	0.07	0.18	0	2	-100%
	0.06	0.15	0	2	-100%
	0.06	0.15	1	0	100%
	0.06	0.15	1	1	0%

8.3 Xylitol

8.3.1 Introduction

Pentane-1,2,3,4,5-pentaol is a polyalcohol with molecular formula $C_5H_{12}O_5$. This pentahydroxy sugar alcohol has three stereoisomers: arabinitol, xylitol, and ribitol (Figure **33**).[145] Arabinitol is a chiral molecule with two enantiomers, L-arabinitol and D-arabinitol. Xylitol and ribitol, on the other hand, are achiral molecules with *meso* configuration and a pseudo-chiral center at C_3.[146] While ribitol crystallizes as a racemate, Xylitol forms enantiopure crystals upon crystallization in an orthorhombic system with space group $P2_12_12_1$.[146] In other words xylitol crystallizes as a conglomerate in the same space group as epsomite.

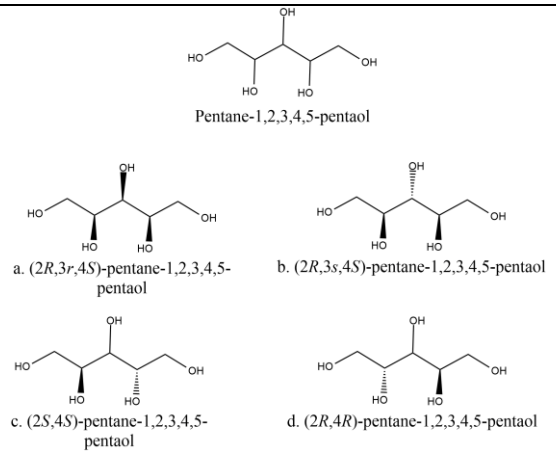

Figure 33. Structures of Stereoisomers of pentane-1,2,3,4,5-pentaol: (a) xylitol, (b) ribitol, (c) L-arabinitol, and (d) D-arabinitol.

The crystalline structure of xylitol was reported for the first time by Wolfrom and Kohn in 1942.[147] According to Kim and Jeffrey (1969), xylitol has enantiomorphic crystal structures when it crystallizes.[146] In

principle, one should be able to investigate the chirality of xylitol crystals in the same way as epsomite. Xylitol crystals were grown and studied, but the chirality of the crystals could not be determined due to symmetry (*i.e.*, absence of a hemihedrism). This absence of asymmetry is often observed when epsomite is grown without chiral/achiral additives. Since xylitol does not contain a chromophore and can be detected by the ultraviolet-visible spectrometer or solid-state circular dichroism, it needs another method for the identity confirmation.

8.3.2 Experimental

Xylitol crystals were grown using two methods: slow evaporation and seeding method. Commercially purchased xylitol (Natural Drop Xylitol amazon.ca) was used in this experiment. Water, 95% ethanol and methanol were used as crystallization solvents. The solubility of xylitol is higher in water (169 g/L), and lower in methanol (6 g/L) and ethanol (1.2 g/L).

The first step in crystal growth was to prepare a saturated solution according (fix) the solubility of xylitol. The saturated solution was prepared by dissolving 169 g of xylitol in 100 mL of distilled water, in a 250 mL beaker at 60℃.[148] Magnetic stirring was used to facilitate dissolution. Complete dissolution was crucial to eliminate any undissolved crystals which can cause secondary nucleation to occur. The warm solution was poured into a glass petri dish and four 100 mL beakers and allowed to cool to room temperature. The solutions in the 100 mL beakers were covered with plastic wrap with small holes to lower the rate of evaporation while the glass petri dish was left open to obtain more seed crystals. The solutions were kept in an undisturbed environment at room temperature to minimize secondary nucleation. The temperature inside the laboratory was around 24℃.

Seed crystals were collected from the solution in the glass petri dish after 12 to 15 hours using tweezers. After the seeds were taken out of the solution, they were dried using Kimwipes® to prevent further nucleation. The seed crystals, around 4 mm in size, were tied using a very fine nylon cord with a slip knot and were suspended in a saturated solution prepared as described above. Seeds were suspended after the solution cooled to room temperature to prevent the seeds from dissolving after suspension. The other end of the string was twisted on a pencil and placed on top of the beaker. The beaker was covered with plastic wrap for slow solvent evaporation.

Single xylitol crystals from slow evaporation beakers were typically collected 14 to 30 days after initial preparation. The single crystals were wiped using Kimwipes® to remove excess solution on the surface of the crystals. Suspended crystals were typically taken out of the solution between 7 to 14 days after initial suspension.

Xylitol crystal growth in 95% ethanol was also performed by dissolving 1.2 g of xylitol in 100 mL of 95% ethanol in a 100 mL beaker at 60℃. Since ethanol is very volatile, the beaker was covered with a watch glass to prevent fast evaporation of the solvent. After complete dissolution, the solution was cooled and covered with plastic wrap. Small holes were made to maintain slow evaporation. The same procedures were followed to grow xylitol crystals in methanol. The saturated solution was prepared by dissolving 6 g of xylitol in 100 mL of methanol. Since ethanol and methanol are volatile solvents, only one or two holes in the plastic wrap were made to allow slow evaporation.

Xylitol crystals were grown in the presence of borax to influence crystal morphology. 2.4 g of borax was added to 50 mL of xylitol solution and dissolved at 60℃. The solution was cooled to room temperature, then covered with a plastic wrap with holes. The solution was kept at room temperature in an undisturbed environment.

8.3.3 Results and Discussion

Xylitol crystals were grown and studied to attempt to determine chirality. Well-developed xylitol crystals were collected from saturated aqueous solutions. These crystals were very symmetric and no hemihedral face was observed. In total, 46 xylitol crystals were collected from many crystallization experiments. These crystals ranged from 8 mm to 27 mm in size, weighed between 0.45 g to 30.6 g, and presented 24 to 27 crystal faces (Figure 34).

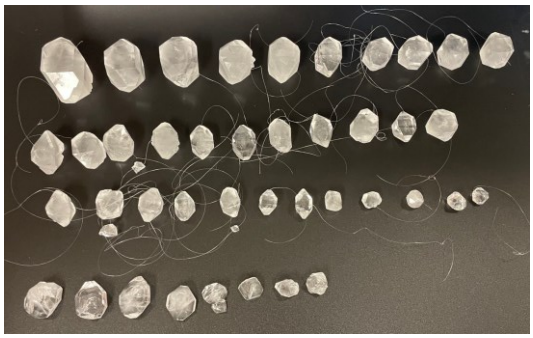

Figure 34. Xylitol crystals grown via slow evaporation and seed suspension techniques.

The 3-dimensional (3D) model of a single xylitol crystal was built using VESTA (version 3). The unit cell parameter was obtained from Crystallography Open Database.[149] The 3D model was built by adjusting the size to resemble the real crystal. The miller indices of the crystal faces were determined using the software (**Figure 35**).

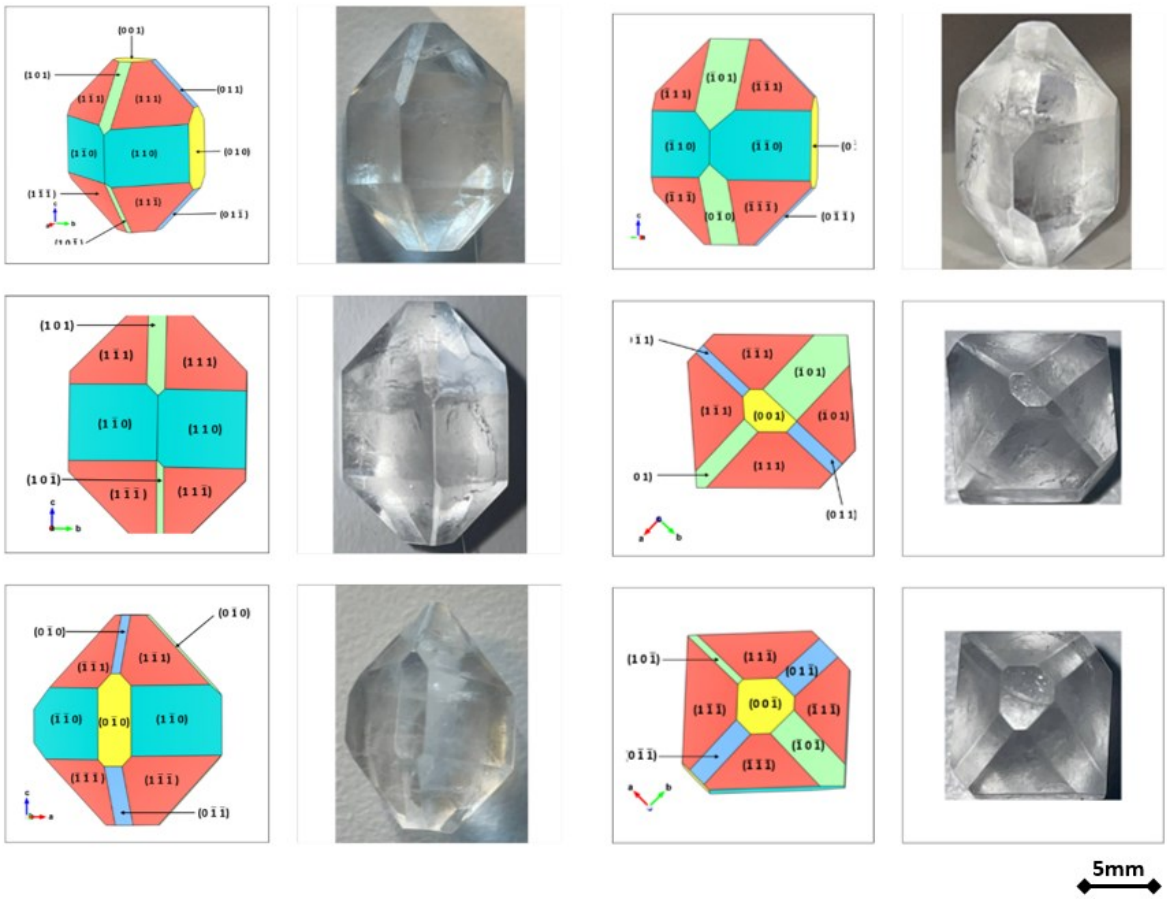

Figure 35. Xylitol Crystal (right) and 3D model (left) from different point of view or perspective.

In addition, the interfacial angles were measured using a contact goniometer and compared with the theoretical interfacial angles obtained from VESTA software. Only interfacial angles of adjacent faces were measured using a contact goniometer.

Table 10. Sample interfacial angle measurement of adjacent faces using contact goniometer and theoretical value obtained from VESTA version 3.

	Face		Theoretical (°)	Measured (°)	
				Crystal 1	Crystal 2
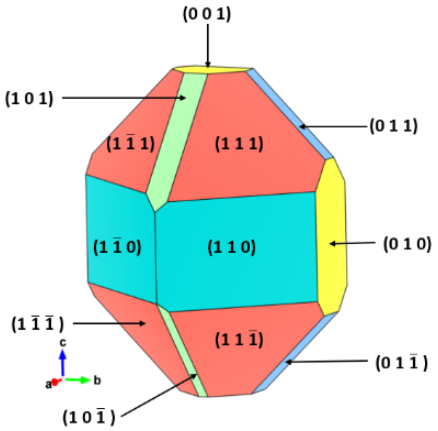	(1 1 0)	($1\bar{1}$ 0)	85.55	83	87
		(1 1 $\bar{1}$)	34.18	34	33
		(1 1 1)	34.18	35	35
		(1 0 1)	57.40	-	56
		(1 0 $\bar{1}$)	57.40	55	54
		(0 1 0)	47.22	47	47
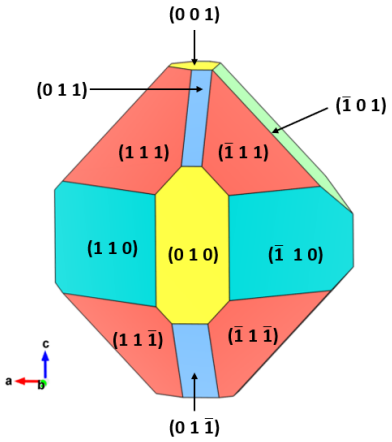	(0 1 0)	($\bar{1}$ 1 1)	55.18	55	56
		(1 1 1)	55.18	55	54
		(1 1 $\bar{1}$)	55.18	56	56
		($\bar{1}$ 1 $\bar{1}$)	55.18	56	55
		(0 1 1)	45.00	45	45
		(0 1 $\bar{1}$)	45.00	45	-
		(1 1 0)	47.22	47	47
		($\bar{1}$ 1 0)	47.22	45	47

In Table 10, the angles give evidence for the presence of symmetry in xylitol. Because of this symmetry or the absence of asymmetric faces, the chirality of xylitol could not be determined as in the case of epsomite.

High quality xylitol crystals could not be grown from ethanol due to the volatility of the solvent. Many xylitol seed crystals with an elongated shape, which were about 0.1 mm in size, were obtained from methanol solution. A single and larger crystal could not be obtained from methanol solution due to the high volatility of methanol, which made slow evaporation more difficult. Furthermore, no change in morphology was observed when borax was used as an additive.

8.3.4 Future work

Although the chirality of xylitol crystal was not determined in this project, future works can be done to determine the crystal chirality. Dye inclusion circular dichroism is a way of incorporating achiral dyes into a chiral crystal. Solid state circular dichroism can be conducted by introducing achiral chromophore molecules to xylitol.